

# An efficient primal dual semismooth Newton method for semidefinite programming

**Zhanwang Deng**

*Academy for Advanced Interdisciplinary Studies*

*Peking University*

*Beijing, 100871, China*

**Jiang Hu\***

DEPARTMENT OF MATHEMATICS,

UNIVERSITY OF CALIFORNIA, BERKELEY,

BERKELEY, CA 94720, US

**Kangkang Deng**

*Department of Mathematics*

*National University of Defense Technology*

*Changsha, 410073, CHINA*

**Zaiwen Wen**

*Beijing International Center for Mathematical Research*

*Center for Machine Learning Research*

*Changsha Institute for Computing and Digital Economy*

*Peking University*

*Beijing 100871, CHINA*

DZW\_OPT2022@STU.PKU.EDU.CN

HUJIANGOPT@GMAIL.COM

FREEDENG1208@GMAIL.COM

WENZW@PKU.EDU.CN

## Abstract

In this paper, we present an efficient semismooth Newton method, named SSNCP, for solving a class of semidefinite programming problems. Our approach is rooted in an equivalent semismooth system derived from the saddle point problem induced by the augmented Lagrangian duality. An additional correction step is incorporated after the semismooth Newton step to ensure that the iterates eventually reside on a manifold where the semismooth system is locally smooth. Global convergence is achieved by carefully designing inexact criteria and leveraging the  $\alpha$ -averaged property to analyze the error. The correction steps address challenges related to the lack of smoothness in local convergence analysis. Leveraging the smoothness established by the correction steps and assuming a local error bound condition, we establish the local superlinear convergence rate without requiring the stringent assumptions of nonsingularity or strict complementarity. Furthermore, we prove that SSNCP converges to an  $\varepsilon$ -stationary point with an iteration complexity of  $\tilde{O}(\varepsilon^{-3/2})$ . Numerical experiments on various datasets, especially the Mittelmann benchmark, demonstrate the high efficiency and robustness of SSNCP compared to state-of-the-art solvers.

**Keywords:** Semidefinite programming, primal dual algorithm, semismooth Newton method, globalization, superlinear convergence.

---

\*. Corresponding author

## 1 Introduction

The goal of this paper is to design an efficient and practical algorithm that is comparable to state-of-the-art solvers for solving the following large-scale convex composite semidefinite programming (SDP) problem:

$$\min \langle \mathbf{c}, \mathbf{x} \rangle + h(\mathbf{x}), \text{ s.t. } \mathcal{A}(\mathbf{x}) \in \mathcal{Q}, \mathbf{x} \in \mathcal{K}, \quad (1)$$

where  $\mathbf{c} \in \mathbb{S}^{n \times n}$ , and  $\mathcal{K} = \mathbb{S}_+^n$  denotes the positive semidefinite cone. The map  $\mathcal{A} : \mathbb{S}^{n \times n} \rightarrow \mathbb{R}^m$  is linear,  $\mathcal{Q}$  represents a box constraint, and  $h$  is an elementwise indicator function on a polyhedral convex set. The function  $h$  provides flexibility to handle additional constraints, such as nonnegative or box constraints. The original problem (1) encompasses both the standard SDP and SDP with nonnegative constraints (SDP+). Although the examples presented in (1) focus on specific SDP problems, the proposed algorithm can handle more general forms of  $h$ , provided that its proximal operator is computationally tractable.

SDP is a fundamental component of classical conic optimization, with extensive applications in diverse domains. This problem class has been the subject of intensive research for several decades and continues to attract significant attention (Zhao et al., 2010; Sun et al., 2020; Wang et al., 2023; de Roux et al., 2025; Tavakoli et al., 2024). For a comprehensive theoretical analysis and an overview of the critical roles of SDP in fields such as finance, engineering, optimal control, statistics, and machine learning, we refer readers to (Anjos and Lasserre, 2011; Wolkowicz et al., 2012). Given its widespread applications in engineering and machine learning, the development of efficient solvers for SDP has emerged as a central focus in the field of optimization in recent decades. We provide a survey of algorithms for solving SDP problems in the following subsection.

### 1.1 Literature review

First-order methods are popular for solving large-scale optimization problems due to the low complexity at each iteration. For SDP and SDP+ problems, the alternating direction method of multipliers (ADMM), as implemented in SDPAD (Wen et al., 2010), has demonstrated considerable numerical efficacy. A two-block decomposition hybrid proximal extragradient method, termed 2EBD, is proposed in (Monteiro et al., 2014). Subsequently, a convergent symmetric Gauss–Seidel based three-block ADMM method is developed in (Sun et al., 2015), which is capable of handling SDP problems with additional polyhedral set constraints. These first-order methods often achieve a low-accuracy solution rapidly but may require many iterations to attain a highly accurate solution. Consequently, further efforts are necessary to enhance their practicality.

The interior point method (Nesterov and Nemirovskii, 1994) is a well-established, efficient classical approach for SDP. This method employs a sequence of log-barrier penalty subproblems, requiring one step of Newton’s method to solve each subproblem. Open-source solvers such as SeDuMi (Sturm, 1999) and SDPT3 (Toh et al., 1999) have been widely adopted. They achieve considerable success in various application domains. Furthermore, commercial solvers based on interior point methods, such as MOSEK (ApS, 2019), are also well-developed. Nevertheless, each step of the interior point method requires a factorization of the Schur complement matrix. When the number of constraints is large, the computational complexity and memory requirements increase significantly, leading to substantially

increased runtime. If iterative methods are employed, the low-rank or high-rank structure of the solution cannot be exploited. Furthermore, when handling SDP with affine constraints, the interior point method needs to introduce extra nonnegative variables to transform the original problem into a conic problem. This transformation will lead to an increase in the scale of the linear systems, thereby requiring more memory.

The decomposition method has also proven to be effective for low-rank SDP. To circumvent the positive semidefinite constraint, Burer and Monteiro (Burer and Monteiro, 2003) recast the linear SDP by factorizing the original variables. They apply the augmented Lagrangian (AL) method and use a quasi-Newton method to solve the factorized subproblem. Recently, a decomposition augmented Lagrangian method for low-rank SDP has been proposed in (Wang et al., 2023). This method utilizes a semismooth Newton method on the manifold to solve the subproblem in the AL method, leveraging the low-rank property. However, the initialization and adjustment of the rank parameter are crucial for the decomposition method. Furthermore, for problems that have high-rank solutions, the decomposition method may not be efficient.

In addition to the methods mentioned above, semismooth Newton methods have also demonstrated effectiveness in addressing large-scale SDP problems. In the context of the AL method, a Newton-CG AL method to solve SDPs, SDPNAL, is proposed in (Zhao et al., 2010). This method is later extended to a MATLAB software package, SDPNAL+, for SDP with bound constraints (Sun et al., 2020). Furthermore, motivated by the equivalence between the Douglas-Rachford splitting (DRS) iteration and the ADMM, a semismooth Newton method based solver, SSNSDP, for SDP problems arising in electronic structure calculations has been proposed (Li et al., 2018). However, its convergence analysis relies on switching between the semismooth Newton method and ADMM. This approach is subsequently generalized to address optimal transport problems (Liu et al., 2022). Recently, a primal dual semismooth Newton method has been proposed for multi-block convex composite optimization problems in (Deng et al., 2025). This method is based on the nonlinear system derived from the AL saddle point problem. However, the strict complementarity (SC) condition is necessary for the convergence analysis, which may not hold in general. This motivates us to design a more practical algorithm with relaxed requirements for superlinear convergence analysis.

## 1.2 Contributions

The contributions of this paper are listed as follows:

(1) Using the AL duality, we transform the original problem (1) into a saddle point problem and formulate a semismooth system of nonlinear equations to characterize the optimality conditions. Different from the construction in (Li et al., 2018) which depends on the DRS iteration for two blocks of composite optimization problems, our reformulation is easily accessible and better suited for handling (1). Subsequently, we develop SSNCP, a regularized semismooth Newton method with nonmonotone line search and carefully designed inexact criteria. Furthermore, to address challenges related to the lack of smoothness in local analysis, an additional correction step is incorporated. Compared with the two loops in the augmented Lagrangian methods (Zhao et al., 2010), our method updates both primal and dual variables in a single semismooth Newton step simultaneously.

(2) We establish the global convergence of SSNCP by carefully designing inexact criteria and leveraging the inherent  $\alpha$ -averaged property to control the error. For the local convergence, thanks to the correction step, the manifold identification of the iteration sequence is proved, namely, iterates eventually reside on a manifold. Consequently, without requiring the stringent nonsingularity or SC assumption, we show that the local smooth transition to the superlinear convergence of the iterate sequences under the error bound condition. Furthermore, the worst iteration complexity of SSNCP is  $\tilde{\mathcal{O}}(\varepsilon^{-3/2})$ . To our knowledge, this is probably the first iteration complexity analysis on semismooth Newton-type algorithms.

(3) Promising and extensive numerical results are presented across various SDP and SDP+ datasets. SSNCP demonstrates superior performance compared to state-of-the-art solvers on all tested problems. Notably, SSNCP is able to compete with MOSEK on challenging Mittelmann benchmark problems. The results indicate that SSNCP is robust and efficient in solving complex and large-scale SDP problems.

### 1.3 Notation

For a linear operator  $\mathcal{A}$ , we denote its adjoint operator by  $\mathcal{A}^*$ . The dual cone of  $\mathcal{K}$  is defined as  $\mathcal{K}^* := \{\mathbf{y} : \langle \mathbf{y}, \mathbf{x} \rangle \geq 0, \forall \mathbf{x} \in \mathcal{K}\}$ . For a proper convex function  $g$ , we define its domain as  $\text{dom}(g) := \{\mathbf{x} : g(\mathbf{x}) < \infty\}$ . The Fenchel conjugate function of  $g$  is  $g^*(\mathbf{z}) := \sup_{\mathbf{x}} \{\langle \mathbf{x}, \mathbf{z} \rangle - g(\mathbf{x})\}$  and the subdifferential is  $\partial g(\mathbf{x}) := \{\mathbf{z} : g(\mathbf{y}) - g(\mathbf{x}) \geq \langle \mathbf{z}, \mathbf{y} - \mathbf{x} \rangle, \forall \mathbf{y}\}$ . For a convex set  $\mathcal{Q}$ , we use  $\delta_{\mathcal{Q}}$  to denote its indicator function, which takes value 0 on  $\mathcal{Q}$  and  $+\infty$  elsewhere. The relative interior of  $\mathcal{Q}$  is denoted by  $\text{ri}(\mathcal{Q})$  and the boundary of  $\mathcal{Q}$  is denoted by  $\text{bd}(\mathcal{Q})$ . The projection operator onto a closed convex set  $\mathcal{C}$  is defined by  $\Pi_{\mathcal{C}}(\mathbf{x}) = \arg \min_{\mathbf{y} \in \mathcal{C}} \|\mathbf{y} - \mathbf{x}\|^2$ . For any proper closed convex function  $g$ , and constant  $t > 0$ , the proximal operator of  $g$  is defined by  $\text{prox}_{tg}(\mathbf{x}) = \arg \min_{\mathbf{y}} \{g(\mathbf{y}) + \frac{1}{2t} \|\mathbf{y} - \mathbf{x}\|^2\}$ . The notion  $n_1 = \mathcal{O}(n)$  means there exists a constant  $C$  such that  $n_1 \leq Cn$  and  $\tilde{\mathcal{O}}$  indicates that logarithmic factors of  $\mathcal{O}$  are ignored.

### 1.4 Organization

The rest of this paper is organized as follows. In Section 2, we present a nonlinear system characterization of the optimality condition of (1) based on the AL saddle point, under the assumption of Slater's condition to ensure strong duality. In Section 3, we propose a semismooth Newton method to solve problem (1). Theoretical analysis, including global and local convergence as well as iteration complexity, is established in Section 4. Extensive numerical experiments are presented in Section 5 and we conclude this paper in Section 6.

## 2 Preliminaries

In this section, we first transform the original problem (1) into a saddle point problem using the AL duality. A monotone nonlinear system derived from the saddle point problem is then presented and analyzed. Furthermore, under mild assumptions on the proximal operator of  $h$ , such a nonlinear system can be semismooth and equivalent to the Karush–Kuhn–Tucker (KKT) optimality condition of problem (1).

## 2.1 An equivalent saddle point problem

In this subsection, we present the construction of the saddle point problem. First, the dual problem of (1) is given by

$$\begin{aligned} \min_{\mathbf{y}, \mathbf{z}, \mathbf{s}} \quad & h^*(-\mathbf{z}) + \delta_{\mathcal{Q}}^*(-\mathbf{y}) + \delta_{\mathcal{K}}^*(-\mathbf{s}), \\ \text{s.t.} \quad & \mathcal{A}^*(\mathbf{y}) + \mathbf{s} + \mathbf{z} = \mathbf{c}, \end{aligned} \quad (2)$$

where  $\mathbf{y} \in \mathbb{R}^m$ ,  $\mathbf{s} \in \mathbb{S}^n$ ,  $\mathbf{z} \in \mathbb{S}^n$ . Throughout this paper, we make the following assumption.

**Assumption 1** *The dual problem (2) has an optimal solution  $\mathbf{y}_*$ ,  $\mathbf{z}_*$ ,  $\mathbf{s}_*$ . Furthermore, Slater's condition holds for the dual problem (2), i.e., there exist  $-\mathbf{y} \in \text{ri}(\text{dom}(\delta_{\mathcal{Q}}^*))$ ,  $-\mathbf{s} \in \text{ri}(\text{dom}(\delta_{\mathcal{K}}^*))$ , and  $-\mathbf{z} \in \text{ri}(\text{dom}(h^*))$  such that  $\mathcal{A}^*(\mathbf{y}) + \mathbf{s} + \mathbf{z} = \mathbf{c}$ .*

Under Assumption 1, the optimal solution  $(\mathbf{y}_*, \mathbf{z}_*, \mathbf{s}_*, \mathbf{x}_*)$  of the primal problem (1) and the dual problem (2) satisfies the following KKT optimality conditions (Karush, 1939; Kuhn and Tucker, 2014):

$$\begin{aligned} 0 &= \mathcal{A}^*(\mathbf{y}_*) + \mathbf{s}_* + \mathbf{z}_* - \mathbf{c}, \quad 0 = \mathcal{A}\mathbf{x}_* - \Pi_{\mathcal{Q}}(\mathcal{A}\mathbf{x}_* - \mathbf{y}_*), \\ 0 &= \mathbf{x}_* - \Pi_{\mathcal{K}}(\mathbf{x}_* - \mathbf{s}_*), \quad \mathbf{x}_* = \text{prox}_h(\mathbf{x}_* - \mathbf{z}_*). \end{aligned} \quad (3)$$

To reformulate the above set-valued KKT system into a single-valued semismooth system, a modified AL function and the associated saddle point problem are introduced in (Deng et al., 2025). We first introduce two auxiliary variables  $\mathbf{v}, \mathbf{p}$  to decouple the variables for the constraint  $\mathcal{A}^*(\mathbf{y}) + \mathbf{s} + \mathbf{z} = \mathbf{c}$  from the possibly nonsmooth term  $h^*$  and the function  $\delta_{\mathcal{Q}}^*$ . By associating Lagrangian multipliers  $(\mathbf{x}, \mathbf{u}, \mathbf{q})$  to the nonsmooth term  $h^*$ ,  $\delta_{\mathcal{Q}}^*$ , and  $\delta_{\mathcal{K}}^*$ , and replacing  $\mathbf{v}, \mathbf{p}$ , and  $\mathbf{s}$  with their closed-form solutions, the modified AL function of (2) is given by

$$\begin{aligned} \Phi(\mathbf{y}, \mathbf{z}, \mathbf{x}, \mathbf{u}, \mathbf{q}) &= \underbrace{h^*(\text{prox}_{h^*/\sigma}(\mathbf{q}/\sigma - \mathbf{z})) + \frac{1}{2\sigma} \|\text{prox}_{\sigma h}(\mathbf{q} - \sigma \mathbf{z})\|^2}_{\text{Moreau envelope of } h^*} \\ &\quad + \underbrace{\frac{1}{2\sigma} \|\Pi_{\mathcal{K}}(\mathbf{x} + \sigma(\mathcal{A}^*(\mathbf{y}) + \mathbf{z} - \mathbf{c}))\|^2}_{\text{Moreau envelope of } \delta_{\mathcal{K}}^*} \\ &\quad + \underbrace{\frac{1}{2\sigma} \|\Pi_{\mathcal{Q}}(\mathbf{u} - \sigma \mathbf{y})\|^2}_{\text{Moreau envelope of } \delta_{\mathcal{Q}}^*} - \frac{1}{2\sigma} (\|\mathbf{x}\|^2 + \|\mathbf{u}\|^2 + \|\mathbf{q}\|^2), \end{aligned} \quad (4)$$

where  $\sigma > 0$  is the penalty parameter. The Moreau envelope for  $h^*$  is defined by:  $e_{\sigma}h^*(\mathbf{x}) := \min_{\mathbf{y}} h^*(\mathbf{y}) + \frac{\sigma}{2} \|\mathbf{y} - \mathbf{x}\|^2$ . The Moreau envelopes  $e_{\sigma}\delta_{\mathcal{Q}}^*$  and  $e_{\sigma}\delta_{\mathcal{K}}^*$  can be defined similarly. Then the corresponding saddle point problem associated with the above AL function is

$$\min_{\mathbf{y}, \mathbf{z}} \max_{\mathbf{x}, \mathbf{u}, \mathbf{q}} \Phi(\mathbf{y}, \mathbf{z}, \mathbf{x}, \mathbf{u}, \mathbf{q}). \quad (5)$$

Denote  $\mathbf{w} := (\mathbf{y}, \mathbf{z}, \mathbf{x}, \mathbf{u}, \mathbf{q})$ . Similar to (Deng et al., 2025, Lemma 2.1), we next give the strong AL duality of  $\Phi(\mathbf{w})$  without proof.

**Lemma 1** *Suppose that Assumption 1 holds. Given  $\sigma > 0$ , the strong duality holds for (5), i.e.,*

$$\min_{\mathbf{y}, \mathbf{z}} \max_{\mathbf{x}, \mathbf{u}, \mathbf{q}} \Phi(\mathbf{y}, \mathbf{z}, \mathbf{x}, \mathbf{u}, \mathbf{q}) = \max_{\mathbf{x}, \mathbf{u}, \mathbf{q}} \min_{\mathbf{y}, \mathbf{z}} \Phi(\mathbf{y}, \mathbf{z}, \mathbf{x}, \mathbf{u}, \mathbf{q}), \quad (6)$$

where both sides of (6) are equivalent to problem (2).

## 2.2 A monotone nonlinear system

In this subsection, we present and analyze the nonlinear system induced from the saddle point problem (5). It follows from the Moreau envelope theorem (Beck, 2017) that  $e_\sigma h^*$ ,  $e_\sigma \delta_Q^*$ , and  $e_\sigma \delta_K^*$  are continuously differentiable, which implies that  $\Phi$  is also continuously differentiable. The gradient of function  $\Phi$  in (4) is given by:

$$\begin{aligned} \nabla_{\mathbf{y}} \Phi(\mathbf{w}) &= \mathcal{A} \Pi_K(\sigma(\mathcal{A}^*(\mathbf{y}) + \mathbf{z} - \mathbf{c}) + \mathbf{x}) - \Pi_Q(\mathbf{u} - \sigma \mathbf{y}), \\ \nabla_{\mathbf{z}} \Phi(\mathbf{w}) &= \Pi_K(\sigma(\mathcal{A}^*(\mathbf{y}) + \mathbf{z} - \mathbf{c}) + \mathbf{x}) - \text{prox}_{\sigma h}(\mathbf{q} - \sigma \mathbf{z}), \\ \nabla_{\mathbf{x}} \Phi(\mathbf{w}) &= -\frac{1}{\sigma} \mathbf{x} + \frac{1}{\sigma} \Pi_K(\sigma(\mathcal{A}^*(\mathbf{y}) + \mathbf{z} - \mathbf{c}) + \mathbf{x}), \\ \nabla_{\mathbf{u}} \Phi(\mathbf{w}) &= -\frac{1}{\sigma} \mathbf{u} + \frac{1}{\sigma} \Pi_Q(\mathbf{u} - \sigma \mathbf{y}), \\ \nabla_{\mathbf{q}} \Phi(\mathbf{w}) &= -\frac{1}{\sigma} \mathbf{q} + \frac{1}{\sigma} \text{prox}_{\sigma h}(\mathbf{q} - \sigma \mathbf{z}). \end{aligned} \quad (7)$$

We focus on the following nonlinear operator

$$F(\mathbf{w}) := (\nabla_{\mathbf{y}} \Phi(\mathbf{w})^\top, \nabla_{\mathbf{z}} \Phi(\mathbf{w})^\top, -\nabla_{\mathbf{x}} \Phi(\mathbf{w})^\top, -\nabla_{\mathbf{u}} \Phi(\mathbf{w})^\top, -\nabla_{\mathbf{q}} \Phi(\mathbf{w})^\top)^\top. \quad (8)$$

It follows from (Deng et al., 2025, Lemma 2.5) that  $\mathbf{w}_*$  is a solution of the saddle point problem (5) if and only if it satisfies  $F(\mathbf{w}_*) = 0$ . Consequently, we can solve  $F(\mathbf{w}) = 0$  to find the solution of the original problem (1). Before analyzing the properties of  $F$ , we give the definition of the Clarke subdifferential and semismoothness, which will play an important role in the subsequent analysis.

**Definition 2** *Let  $F$  be a locally Lipschitz continuous mapping. Denote by  $D_F$  the set of differentiable points of  $F$ . The B-Jacobian of  $F$  at  $\mathbf{w}$  is defined by*

$$\partial_B F(\mathbf{w}) := \left\{ \lim_{k \rightarrow \infty} J(\mathbf{w}^k) \mid \mathbf{w}^k \in D_F, \mathbf{w}^k \rightarrow \mathbf{w} \right\},$$

where  $J(\mathbf{w})$  denotes the Jacobian of  $F$  at  $\mathbf{w} \in D_F$ . The set  $\partial F(\mathbf{w}) = \text{co}(\partial_B F(\mathbf{w}))$  is called the Clarke subdifferential, where  $\text{co}$  denotes the convex hull.

The mapping  $F$  is called *semismooth* at  $\mathbf{w}$  if  $F$  is directionally differentiable at  $\mathbf{w}$  and for any  $\mathbf{d}$ ,  $J \in \partial F(\mathbf{w} + \mathbf{d})$ , it holds that  $\|F(\mathbf{w} + \mathbf{d}) - F(\mathbf{w}) - J\mathbf{d}\| = o(\|\mathbf{d}\|)$ ,  $\mathbf{d} \rightarrow 0$ . Moreover,  $F$  is said to be *strongly semismooth* at  $\mathbf{w}$  if  $F$  is directionally differentiable at  $\mathbf{w}$  and  $\|F(\mathbf{w} + \mathbf{d}) - F(\mathbf{w}) - J\mathbf{d}\| = O(\|\mathbf{d}\|^2)$ ,  $\mathbf{d} \rightarrow 0$ . We say  $F$  is *semismooth* (respectively, *strongly semismooth*) if  $F$  is *semismooth* (respectively, *strongly semismooth*) for any  $\mathbf{w}$  (Mifflin, 1977).

By (Deng et al., 2025, Lemma 2), we know that  $F$  is always monotone, and it is semismooth if  $\text{prox}_h$  is semismooth. Unlike the semismooth system constructed in the AL method (Zhao et al., 2010) that relies on the knowledge of the multipliers, our approach implies the optimality conditions directly. Furthermore, although there are other potential ways to construct semismooth systems induced from the KKT conditions (Liang et al., 2023), the resulting systems are generally nonmonotone and even nonsymmetric. Such nonmonotonicity can raise some practical and theoretical issues including the lack of globalization. In contrast, our approach to constructing the semismooth system is more unified and does not depend on the integration of first-order methods (Li et al., 2018; Xiao et al., 2018a).

### 3 An efficient semismooth Newton method

In this section, we present a semismooth Newton algorithm to solve  $F(\mathbf{w}) = 0$ .

#### 3.1 Generalized Jacobian of $F$

We first present the generalized Jacobian operator of  $F$ . Denote

$$\begin{aligned}\partial\Pi_{\mathcal{Q}} &:= \partial\Pi_{\mathcal{Q}}(\mathbf{u} - \sigma\mathbf{y}), \quad \partial\text{prox}_h := \partial\text{prox}_{\sigma h}(\mathbf{q} - \sigma\mathbf{z}), \\ \partial\Pi_{\mathcal{K}} &:= \partial\Pi_{\mathcal{K}}(\sigma(\mathcal{A}^*(\mathbf{y}) + \mathbf{z} - \mathbf{c}) + \mathbf{x})\end{aligned}$$

as the Clarke subdifferentials of  $\Pi_{\mathcal{Q}}$ ,  $\text{prox}_{\sigma h}$  and  $\Pi_{\mathcal{K}}$  at  $\mathbf{u} - \sigma\mathbf{y}$ ,  $\mathbf{q} - \sigma\mathbf{z}$ ,  $\mathbf{x} + \sigma(\mathcal{A}^*(\mathbf{y}) + \mathbf{z} - \mathbf{c})$ , respectively. We also define the following matrix operators:

$$\mathcal{H}_1 = \begin{pmatrix} \sigma(D_{\mathcal{Q}} + \mathcal{A}D_{\mathcal{K}}\mathcal{A}^*) & \sigma\mathcal{A}D_{\mathcal{K}} \\ \sigma D_{\mathcal{K}}\mathcal{A}^* & \sigma(D_h + D_{\mathcal{K}}) \end{pmatrix}, \quad \mathcal{H}_2 = \begin{pmatrix} -\mathcal{A}D_{\mathcal{K}} & D_{\mathcal{Q}} & 0 \\ -D_{\mathcal{K}} & 0 & D_h \end{pmatrix}, \quad (9)$$

and

$$\mathcal{H}_3 = \text{blkdiag} \left\{ \frac{1}{\sigma}(I - D_{\mathcal{K}}), \frac{1}{\sigma}(I - D_{\mathcal{Q}}), \frac{1}{\sigma}(I - D_h) \right\},$$

where  $\text{blkdiag}$  denotes the block diagonal matrix operator,  $D_{\mathcal{Q}} \in \partial\Pi_{\mathcal{Q}}$ ,  $D_h \in \partial\text{prox}_h$ , and  $D_{\mathcal{K}} \in \partial\Pi_{\mathcal{K}}$ . For any  $\mathbf{w}$ , define

$$\hat{\partial}F(\mathbf{w}) := \left\{ \begin{pmatrix} \mathcal{H}_1 & \mathcal{H}_2 \\ -\mathcal{H}_2^\top & \mathcal{H}_3 \end{pmatrix} : \text{where } \mathcal{H}_1, \mathcal{H}_2, \text{ and } \mathcal{H}_3 \text{ are defined in (9)} \right\}. \quad (10)$$

It follows from (Hiriart-Urruty et al., 1984) and the definition of  $\hat{\partial}F$  that  $\hat{\partial}F(\mathbf{w})[\mathbf{d}] = \partial F(\mathbf{w})[\mathbf{d}]$  for any  $\mathbf{d}$ . Hence,  $\hat{\partial}F(\mathbf{w})$  can be used to construct the Newton equation for solving  $F(\mathbf{w}) = 0$ .

#### 3.2 A correction step

To address the challenge related to the lack of smoothness, we propose a correction step. Specifically, we define

$$\begin{aligned}\hat{\mathbf{q}} &:= \arg \min_{\hat{\mathbf{q}}_{i,j} \in \mathcal{C}_{i,j}} \|\mathbf{q} - \hat{\mathbf{q}}\|, & \hat{\mathbf{u}} &:= \arg \min_{\hat{\mathbf{u}}_i \in \text{bd}(\mathcal{Q}_i)} \|\mathbf{u} - \hat{\mathbf{u}}\|, \\ \hat{\mathbf{z}} &:= \arg \min_{\hat{\mathbf{z}}_{i,j} \in -\text{bd}(\partial h_{i,j}(\hat{\mathbf{q}}_{i,j}))} \|\hat{\mathbf{z}} - \mathbf{z}\|, & \hat{\mathbf{y}} &:= \arg \min_{\hat{\mathbf{y}}_i \in -\text{bd}(\mathcal{N}_{\mathcal{Q}_i}(\hat{\mathbf{u}}_i))} \|\hat{\mathbf{y}} - \mathbf{y}\|,\end{aligned} \quad (11)$$

where  $h_{i,j}$  is  $(i,j)$ -th component of  $h$ ,  $\mathcal{Q}_i$  denotes the constraint obtained by restricting the decomposable set  $\mathcal{Q}$  to the  $i$ -th coordinate,  $\mathcal{N}_{\mathcal{Q}_i}$  denotes the normal cone of  $\mathcal{Q}_i$ , and  $\mathcal{C}_{i,j}$  denotes the set of nondifferentiable points of  $h_{i,j}$ . It can be seen that  $\hat{\mathbf{q}}_{i,j}$  and  $\hat{\mathbf{u}}_{i,j}$  correspond to the orthogonal projections of  $\mathbf{q}_{i,j}$  and  $\mathbf{u}_{i,j}$  onto the nondifferentiable points of  $h_{i,j}$  and  $\text{bd}(\mathcal{Q}_i)$ , respectively. Analogously,  $\hat{\mathbf{z}}_{i,j}$  and  $\hat{\mathbf{y}}_i$  are the orthogonal projections of  $\mathbf{z}_{i,j}$  and  $\mathbf{y}_i$  onto the boundaries of 1-dimensional sets  $-\partial h_{i,j}(\hat{\mathbf{q}}_{i,j})$  and  $-\mathcal{N}_{\mathcal{Q}_i}(\hat{\mathbf{u}}_i)$ , respectively. The values of  $(\hat{\mathbf{q}}, \hat{\mathbf{u}}, \hat{\mathbf{z}}, \hat{\mathbf{y}})$  in (11) can be easily obtained for commonly used  $h$  and  $\mathcal{Q}$ . For example, if  $h(\mathbf{x}) = \delta_{\mathbf{x} \geq 0}(\mathbf{x})$ , it follows that  $\mathcal{C}_{i,j} = \{0\}$ ,  $\text{bd}(\partial h_{i,j}(\hat{\mathbf{q}}_{i,j})) = \{0\}$ . Therefore,  $\hat{\mathbf{q}} = \hat{\mathbf{z}} = \mathbf{0} \in \mathbb{R}^{n \times n}$  by (11).

For given  $\sigma$  and  $\mathbf{w} = (\mathbf{y}, \mathbf{z}, \mathbf{x}, \mathbf{u}, \mathbf{q})$ , we denote  $Q\Lambda Q^*$  as the eigenvalue decomposition of  $\mathbf{x} + \sigma(\mathcal{A}^*(\mathbf{y}) + \mathbf{z} - \mathbf{c})$ ,  $\lambda_i = \Lambda_{i,i}$  as the  $i$ -th eigenvalue, and  $Q_i$  as the associated eigenvector of  $\lambda_i$ . Let  $\mathbf{v} := \mathbf{q} - \hat{\mathbf{q}} - \sigma(\mathbf{z} + \hat{\mathbf{z}})$  and  $\mathbf{v} := \mathbf{u} - \hat{\mathbf{u}} - \sigma(\mathbf{y} + \hat{\mathbf{y}})$ . Combining the definitions of  $(\hat{\mathbf{q}}, \hat{\mathbf{u}}, \hat{\mathbf{z}}, \hat{\mathbf{y}})$  in (11), the correction step with nonnegative constants  $\theta, l$ , and  $\rho$  is constructed as:

$$\tilde{\mathbf{w}} = \mathcal{P}_{\theta,l,\rho,\sigma}(\mathbf{y}, \mathbf{z}, \mathbf{x}, \mathbf{u}, \mathbf{q}) := (\mathbf{y}, \mathbf{z}, \mathbf{x} - \sum_{i \in I_{\mathcal{K}}} \lambda_i Q_i Q_i^*, \mathbf{u} - \sum_{i \in I_{\mathcal{Q}}} \mathbf{v}_i, \mathbf{q} - \sum_{(i,j) \in I_h} \mathbf{v}_{ij}), \quad (12)$$

where

$$I_{\mathcal{K}} := \left\{ i \mid |\lambda_i| < \frac{\theta}{2} \right\}, I_h = \left\{ (i,j) \mid |\mathbf{z}_{i,j} - \hat{\mathbf{z}}_{i,j}| < \frac{l}{2\sigma}, |\mathbf{q}_{i,j} - \hat{\mathbf{q}}_{i,j}| < \frac{l}{2} \right\}, \\ I_{\mathcal{Q}} := \left\{ i \mid \|\mathbf{y}_i - \hat{\mathbf{y}}_i\| \leq \frac{\rho}{2\sigma}, \|\mathbf{u}_i - \hat{\mathbf{u}}_i\| < \frac{\rho}{2} \right\}.$$

To provide a more concise explanation,  $\mathcal{P}_{\theta,l,\rho,\sigma}$  adds a correction term on  $\mathbf{x}$  to threshold the eigenvalues of  $\mathbf{x} + \sigma(\mathcal{A}^*(\mathbf{y}) + \mathbf{z} - \mathbf{c})$  with value  $\theta/2$  on their absolute values. A similar approach has also been adopted in solving nonlinear SDP problems (Feng et al., 2025). The operator also performs truncations on  $\mathbf{u}$  and  $\mathbf{q}$  to ensure that the last two components,  $-\nabla_{\mathbf{u}}\Phi(\mathbf{w})$  and  $-\nabla_{\mathbf{q}}\Phi(\mathbf{w})$ , have desired smoothness within a specified regime. Note that if  $(\theta, l, \rho)$  is zero, then  $\mathcal{P}_{\theta,l,\rho,\sigma}$  reduces to the identity operator. Furthermore, since the Clarke subdifferentials of  $\Pi_{\mathcal{K}}$ ,  $\text{prox}_{\sigma h}$ , and  $\Pi_{\mathcal{Q}}$  are all computed at each step, no additional computations arise when carrying out  $\mathcal{P}_{\theta,l,\rho,\sigma}$  operation.

Essentially speaking, the main idea of  $\mathcal{P}_{\theta,l,\rho,\sigma}$  is to project  $\mathbf{w}$  onto a manifold where  $F$  is locally smooth when  $\mathbf{w}$  is close to the solution set, see Lemma 7 for details. In early iteration, it can be the identity operator. This local smoothness allows us to show the local transition to the superlinear convergence. Note that the local superlinear convergence of the update (14) in (Hu et al., 2025) relies on the SC at the solution point, which does not necessarily hold. Designing a superlinear convergent semismooth Newton method is challenging without assuming the SC and BD regularity of  $F$ .

### 3.3 A globalized semismooth Newton method

To globalize the semismooth Newton method, we adopt a nonmonotone line search strategy on the residual sequence  $\{\|F(\mathbf{w}^k)\|\}$ . Given  $\nu \in (0, 1)$ ,  $\beta \in (1/3, 1]$ , and a fixed integer  $i_{\max} \geq 0$ , we search over  $i = 0, \dots, i_{\max}$  to find a suitable regularization parameter  $\tau_{k,i} = \kappa \gamma^i \|F(\mathbf{w}^k)\|$ , where  $\kappa > 0$  and  $\gamma > 1$  are fixed constants. For each  $i$ , we define the direction  $\mathbf{d}^{k,i}$  as the solution to the linear system

$$(J^k + \tau_{k,i} I) \mathbf{d}^{k,i} = -F(\mathbf{w}^k) + \boldsymbol{\eta}^k, \quad (13)$$



where  $J^k \in \hat{\partial}F(\mathbf{w}^k)$  is defined by (10), and  $\boldsymbol{\eta}^k$  is a residual vector representing the inexactness. We require that there exists a constant  $C_\eta > 0$  such that  $\|\boldsymbol{\eta}^k\| \leq C_\eta k^{-\beta}$ . The corresponding trial point is then defined as

$$\bar{\mathbf{w}}^{k,i} = \mathbf{w}^k + \mathbf{d}^{k,i}. \quad (14)$$

Next, for  $i = 0, \dots, i_{\max}$ , we evaluate whether the candidate update satisfies the non-monotone line search condition:

$$\|F(\bar{\mathbf{w}}^{k,i})\| \leq \nu \max_{\max(1, k-\zeta+1) \leq j \leq k} \|F(\mathbf{w}^j)\| + \varsigma_k, \quad (15)$$

where  $\bar{\mathbf{w}}^{k,i} = \mathcal{P}_{\theta, l, \rho, \sigma}(\bar{\mathbf{w}}^{k,i})$  and  $\{\varsigma_k\}_{k=1}^\infty$  is a nonnegative sequence satisfying  $\sum_{k=1}^\infty \varsigma_k^2 < \infty$ . If (15) is satisfied for some  $i$ , we stop searching  $i$  and set the next iterate as  $\mathbf{w}^{k+1} = \bar{\mathbf{w}}^{k,i}$ . If (15) fails for all  $i \leq i_{\max}$ , we set

$$\tau_{k,i} = \kappa_1 k^\beta, \quad (16)$$

where  $\kappa_1 \geq 1$  is a given constant, and set  $\mathbf{w}^{k+1} = \bar{\mathbf{w}}^{k,i}$  defined in (14). Conditions (15) or (16) require that either the norm of  $F$  evaluated at  $\bar{\mathbf{w}}^{k,i}$  has sufficient decrease property or  $\tau_{k,i}$  is chosen as in (16).

The line search over the regularization parameter ensures that a regularized second-order step is always used. Since the condition (15) is quite loose, the regularized parameter  $\tau_{k,i}$  may not be too large in practice, ensuring that the steps closely approximate exact semismooth Newton steps in most cases. As will be shown later, (15) eventually holds with  $i = 0$  provided certain conditions (e.g., local error bound) are satisfied, which eliminates the need to search over  $i$ . Moreover, superlinear convergence is achieved, and (16) occurs only finite times in this case. In numerical experiments, we also find that in most cases even though  $\|F(\mathbf{w})\|$  may increase in the current step, it will decrease in the next few steps. Consequently, condition (15) is effective and efficient both in theory and numerics.

---

**Algorithm 1** A semismooth Newton method for solving (1)

---

**Input:** The constants  $\kappa_1 > 0$ ,  $\gamma > 1$ ,  $\nu \in (0, 1)$ ,  $\beta \in (1/3, 1]$ ,  $\kappa > 0$ , positive integers  $\zeta, i_{\max}$ , nonnegative sequence  $\{\varsigma_k\}, \{\theta^k\}, \{l^k\}, \{\rho^k\}$ , an initial point  $\mathbf{w}^0$  and set  $k = 0$ .

- 1: **while** *stopping condition not met* **do**
- 2:   Calculate  $F(\mathbf{w}^k)$  and select  $J(\mathbf{w}^k) \in \partial F(\mathbf{w}^k)$ .
- 3:   Find  $\tau_{k,i}$  such that either (15) holds with  $\bar{\mathbf{w}}^{k,i} = \mathcal{P}_{\theta^k, l^k, \rho^k, \sigma}(\bar{\mathbf{w}}^{k,i})$  or (16) holds.
- 4:   Set  $\mathbf{w}^{k+1} = \bar{\mathbf{w}}^{k,i}$  if (15) holds; otherwise, define  $\mathbf{w}^{k+1} = \bar{\mathbf{w}}^{k,i}$  as in (14).
- 5:   Set  $k = k + 1$ .
- 6: **end while**

---

### 3.4 An efficient implementation of Newton step

When Algorithm 1 is applied to solve  $F(\mathbf{w}) = 0$ , the key part is to obtain the search direction  $\mathbf{d}^k$  from the linear system. In this subsection, we show how to solve the linear system efficiently. Let  $\mathbf{d} = (d_y; d_z; d_x; d_u; d_q)$ , which corresponds to the directions of variables  $\mathbf{y}, \mathbf{z}, \mathbf{x}, \mathbf{u}, \mathbf{q}$ , respectively. We consider the following Newton equation:

$$(J^k + \tau_k I) \mathbf{d}^k = -\tilde{F}^k, \quad (17)$$

where  $\tilde{F}^k = F(\mathbf{w}^k) - \boldsymbol{\eta}^k$ . Denote  $D_{\mathcal{K}}^{\tau} = ((\frac{1}{\sigma} + \tau_{\mathbf{x}})\mathcal{I} - \frac{1}{\sigma}D_{\mathcal{K}})$ ,  $\tilde{D}_{\mathcal{K}} = D_{\mathcal{K}}(D_{\mathcal{K}}^{\tau})^{-1}D_{\mathcal{K}}$ .  $D_h^{\tau}, \tilde{D}_h, D_{\mathcal{Q}}^{\tau}$ , and  $\tilde{D}_{\mathcal{Q}}$  can be defined analogously. It follows from the proper, closedness, and convexity of  $h$ ,  $\delta_{\mathcal{Q}}$ , and  $\delta_{\mathcal{K}}$ , that  $\mathcal{I} - D_h$ ,  $\mathcal{I} - D_{\mathcal{Q}}$ , and  $\mathcal{I} - D_{\mathcal{K}}$  are positive semidefinite (Milzarek, 2016, Lemma 3.3.5), implying that  $D_h^{\tau}$ ,  $D_{\mathcal{Q}}^{\tau}$ , and  $D_{\mathcal{K}}^{\tau}$  are nonsingular.

After Gaussian elimination and ignoring superscript  $k$ , if  $d_{\mathbf{y}}$  and  $d_{\mathbf{z}}$  are obtained, one can compute the explicit solution of  $d_{\mathbf{x}}, d_{\mathbf{u}}, d_{\mathbf{q}}$  by:

$$\begin{aligned} d_{\mathbf{x}} &= (D_{\mathcal{K}}^{\tau_{\mathbf{x}}})^{-1}(-D_{\mathcal{K}}\mathcal{A}^*d_{\mathbf{y}} - D_{\mathcal{K}}d_{\mathbf{z}} - \tilde{F}_{\mathbf{x}}), \\ d_{\mathbf{u}} &= (D_{\mathcal{Q}}^{\tau_{\mathbf{u}}})^{-1}(D_{\mathcal{Q}}d_{\mathbf{y}} - \tilde{F}_{\mathbf{u}}), \quad d_{\mathbf{q}} = (D_h^{\tau_{\mathbf{q}}})^{-1}(D_h d_{\mathbf{z}} - \tilde{F}_{\mathbf{q}}). \end{aligned} \quad (18)$$

Then, the linear system (17) is reduced to

$$\begin{pmatrix} \mathcal{M}_1 & \mathcal{M}_2 \\ \mathcal{M}_3 & \mathcal{M}_4 \end{pmatrix} \begin{pmatrix} d_{\mathbf{y}} \\ d_{\mathbf{z}} \end{pmatrix} = \begin{pmatrix} \tilde{R}_{\mathbf{y}} \\ \tilde{R}_{\mathbf{z}} \end{pmatrix}, \quad (19)$$

where

$$\begin{aligned} \mathcal{M}_1 &= \overline{D}_{\mathcal{Q}} + \tau_{\mathbf{y}}\mathcal{I} + \mathcal{A}\overline{D}_{\mathcal{K}}\mathcal{A}^*, \quad \mathcal{M}_2 = \mathcal{A}\overline{D}_{\mathcal{K}}, \quad \mathcal{M}_3 = \overline{D}_{\mathcal{K}}\mathcal{A}^*, \quad \mathcal{M}_4 = \tau_{\mathbf{z}}\mathcal{I} + \overline{D}_h + \overline{D}_{\mathcal{K}}, \\ \overline{D}_{\mathcal{K}} &= \sigma D_{\mathcal{K}} + \tilde{D}_{\mathcal{K}}, \quad \overline{D}_h = \sigma D_h + \tilde{D}_h, \quad \overline{D}_{\mathcal{Q}} = \sigma D_{\mathcal{Q}} + \tilde{D}_{\mathcal{Q}}, \\ \tilde{R}_{\mathbf{y}} &= -\mathcal{A}D_{\mathcal{K}}(D_{\mathcal{K}}^{\tau})^{-1}\tilde{F}_{\mathbf{x}} + D_{\mathcal{Q}}(D_{\mathcal{Q}}^{\tau})^{-1}\tilde{F}_{\mathbf{u}}(\mathbf{w}) - \tilde{F}_{\mathbf{y}}, \\ \tilde{R}_{\mathbf{z}} &= -D_{\mathcal{K}}(D_{\mathcal{K}}^{\tau})^{-1}\tilde{F}_{\mathbf{x}} + D_h(D_h^{\tau})^{-1}\tilde{F}_{\mathbf{q}} - \tilde{F}_{\mathbf{z}}. \end{aligned}$$

Specifically, the explicit formulation of equation (19) can be represented by:

$$\left[ \begin{pmatrix} \tau_{\mathbf{y}}\mathcal{I} + \overline{D}_{\mathcal{Q}} & 0 \\ 0 & \tau_{\mathbf{z}}\mathcal{I} + \overline{D}_h \end{pmatrix} + \begin{pmatrix} \mathcal{A} \\ \mathcal{I} \end{pmatrix} \overline{D}_{\mathcal{K}}(\mathcal{A}^*, \mathcal{I}) \right] \begin{pmatrix} d_{\mathbf{y}} \\ d_{\mathbf{z}} \end{pmatrix} = \begin{pmatrix} \tilde{R}_{\mathbf{y}} \\ \tilde{R}_{\mathbf{z}} \end{pmatrix}. \quad (20)$$

It follows from the definition of  $D_{\mathcal{Q}}$  that

$$(D_{\mathcal{Q}})_i = \begin{cases} 1, & \text{if } (\mathbf{u} - \sigma\mathbf{y})_i \in \mathcal{Q}_i, \\ 0, & \text{else.} \end{cases}$$

Since  $h$  is an elementwise function,  $D_h$  is also elementwise. Hence, the main computation is to calculate  $\overline{D}_{\mathcal{K}}(\mathcal{A}^*d_{\mathbf{y}} + d_{\mathbf{z}})$  once for every matrix-vector operation.

Let  $\mathbf{y}, \mathbf{z}$  and  $\mathbf{x}$  be fixed. Consider the following eigenvalue decomposition:

$$\mathbf{x} + \sigma(\mathcal{A}^*(\mathbf{y}) + \mathbf{z} - \mathbf{c}) = Q\Gamma_{\mathbf{y}}Q^{\text{T}}, \quad (21)$$

where  $\Gamma_{\mathbf{y}}$  is the diagonal matrix of eigenvalues and  $Q \in \mathbb{R}^{n \times n}$  is the eigenvector matrix. The diagonal elements of  $\Gamma_{\mathbf{y}}$  are arranged in the nonincreasing order:  $\lambda_1 \geq \lambda_2 \geq \dots \geq \lambda_n$ . Define the following index sets  $\alpha := \{i \mid \lambda_i > 0\}$ ,  $\bar{\alpha} := \{i \mid \lambda_i \leq 0\}$ . Then we have that the operator  $D_{\mathcal{K}} : \mathbb{S}^n \rightarrow \mathbb{S}^n$  satisfies

$$D_{\mathcal{K}}(H) := Q(\Sigma \circ (Q^{\text{T}}HQ))Q^{\text{T}}, \quad H \in \mathbb{S}^n,$$

where  $\circ$  denotes the Hadamard product of two matrices and

$$\Sigma = \begin{bmatrix} E_{\alpha\alpha} & v_{\alpha\bar{\alpha}} \\ v_{\alpha\bar{\alpha}}^{\text{T}} & 0 \end{bmatrix}, \quad v_{ij} := \frac{\lambda_i}{\lambda_i - \lambda_j}, \quad i \in \alpha, \quad j \in \bar{\alpha}, \quad (22)$$

where  $E_{\alpha\alpha} \in \mathbb{S}^{|\alpha|}$  is the matrix of ones. Note that the matrix form of  $D_{\mathcal{K}}$  can be expressed as:  $\mathbf{mat}(D_{\mathcal{K}}) = \tilde{Q}\Lambda\tilde{Q}^T$ , where  $\mathbf{mat}$  denotes the matrix form of the operator,  $\tilde{Q} = Q \otimes Q$ ,  $\Lambda = \text{diag}(\text{vec}(\Sigma))$ . Consequently, we have  $\mathcal{A}\bar{D}_{\mathcal{K}}\mathcal{A}^*d_{\mathbf{y}} = \mathcal{A}Q((\bar{\Sigma}) \circ (Q^T(\mathcal{A}^*d_{\mathbf{y}})Q))Q^T$ , where

$$\bar{\Sigma} := \begin{bmatrix} \frac{(1+\sigma\tau_{\mathbf{x}})}{\tau_{\mathbf{x}}}E_{\alpha\alpha} & l_{\alpha\bar{\alpha}} \\ l_{\alpha\bar{\alpha}}^T & 0 \end{bmatrix}, \quad l_{ij} := \frac{\sigma(\sigma\tau_{\mathbf{x}}+1)v_{ij}}{1+\sigma\tau_{\mathbf{x}}-v_{ij}}. \quad (23)$$

Note that  $Y$  can be represented by:

$$Y = [Q_{\alpha} Q_{\bar{\alpha}}] \begin{bmatrix} \frac{1}{\tau_{\mathbf{x}}}Q_{\alpha}^T D_{\mathcal{K}} Q_{\alpha} & \nu_{\alpha\bar{\alpha}} \circ (Q_{\alpha}^T D_{\mathcal{K}} Q_{\bar{\alpha}}) \\ \nu_{\alpha\bar{\alpha}}^T \circ (Q_{\bar{\alpha}}^T D_{\mathcal{K}} Q_{\alpha}) & 0 \end{bmatrix} \begin{bmatrix} Q_{\alpha}^T \\ Q_{\bar{\alpha}}^T \end{bmatrix} = H + H^T,$$

where  $H = Q_{\alpha}[\frac{1}{2\tau_{\mathbf{x}}}(UQ_{\alpha})Q_{\alpha}^T + (\nu_{\alpha\bar{\alpha}}) \circ (UQ_{\bar{\alpha}})Q_{\bar{\alpha}}^T]$  with  $U = Q_{\alpha}^T D_{\mathcal{K}}$ . If  $\alpha > \frac{n}{2}$ , by letting  $Y = \frac{1}{\tau_{\mathbf{x}}}D_{\mathcal{K}} - Q((\frac{1}{\tau_{\mathbf{x}}}E - \Omega) \circ (Q^T D_{\mathcal{K}} Q))Q^T$ , the high rank property can also be used. Hence,  $Y$  can be computed in at most  $8 \min\{|\alpha|, |\bar{\alpha}|\}n^2$  flops. The linear system (20) can be efficiently solved to obtain  $d_{\mathbf{y}}$ ,  $d_{\mathbf{z}}$ . Note that the following identity holds:

$$(D_{\mathcal{K}}^{\tau_{\mathbf{x}}})^{-1} = ((\frac{1}{\sigma} + \tau_{\mathbf{x}})I - \frac{1}{\sigma}D_{\mathcal{K}})^{-1} = \frac{\sigma}{1+\sigma\tau_{\mathbf{x}}}I + \frac{1}{1+\sigma\tau_{\mathbf{x}}}T, \quad (24)$$

where  $T = \tilde{Q}L\tilde{Q}^T$  and  $L_{ii} = \frac{\sigma\lambda_i}{1+\sigma\tau_{\mathbf{x}}-\lambda_i}$ . Then, it follows that:

$$(D_{\mathcal{K}}^{\tau_{\mathbf{x}}})^{-1}(H) = Q(\Sigma_{\tau_{\mathbf{x}}} \circ (Q^T H Q))Q^T = \frac{\sigma}{1+\sigma\tau_{\mathbf{x}}}H + \frac{1}{1+\sigma\tau_{\mathbf{x}}}Q(\Sigma_T \circ (Q^T H Q))Q^T,$$

where  $\Sigma_T = \begin{bmatrix} \frac{1}{\tau_{\mathbf{x}}}E_{\alpha\alpha} & k_{\alpha\bar{\alpha}} \\ k_{\alpha\bar{\alpha}}^T & 0 \end{bmatrix}$ ,  $k_{ij} := \frac{\sigma v_{ij}}{1+\sigma\tau_{\mathbf{x}}-v_{ij}}$ . Consequently, the low-rank or high-rank property can also be used when computing  $d_{\mathbf{x}}$ .

For the standard SDP problem, since the corresponding problem involves only variables  $\mathbf{y}$  and  $\mathbf{s}$ , it follows that  $\mathbf{w}$  and  $\varphi(\mathbf{w})$  reduce to  $(\mathbf{y}, \mathbf{x})$  and  $\Pi_{\mathcal{K}}(\mathcal{A}^*(\mathbf{y}) - \mathbf{c} + \frac{1}{\sigma}\mathbf{x})$ , respectively. The corresponding Newton system is reduced to:

$$\begin{pmatrix} \mathcal{N}_1 & \mathcal{N}_2 \\ \mathcal{N}_3 & \mathcal{N}_4 \end{pmatrix} \begin{pmatrix} d_{\mathbf{y}} \\ d_{\mathbf{x}} \end{pmatrix} = \begin{pmatrix} -\tilde{F}_{\mathbf{y}} \\ -\tilde{F}_{\mathbf{x}} \end{pmatrix}, \quad (25)$$

where  $d_{\mathbf{y}} \in \mathbb{R}^m$ ,  $d_{\mathbf{x}} \in \mathbb{R}^{n \times n}$ .  $\mathcal{N}_1 = \sigma\mathcal{A}D_{\mathcal{K}}\mathcal{A}^* + \tau_{\mathbf{y}}I$ ,  $\mathcal{N}_2 = \mathcal{A}D_{\mathcal{K}}$ ,  $\mathcal{N}_3 = -D_{\mathcal{K}}\mathcal{A}^*$ ,  $\mathcal{N}_4 = \frac{1}{\sigma}(I - D_{\mathcal{K}}) + \tau_{\mathbf{x}}I = D_{\mathcal{K}}^{\tau_{\mathbf{x}}}$ ,  $\tilde{F}_{\mathbf{y}} = -\mathbf{b} + \sigma\mathcal{A}\varphi(\mathbf{w}) - \boldsymbol{\eta}_{\mathbf{y}}$  and  $\tilde{F}_{\mathbf{x}} = -\varphi(\mathbf{w}) + \frac{1}{\sigma}\mathbf{x} - \boldsymbol{\eta}_{\mathbf{x}}$ . Consequently, we only need to solve the following equation corresponding to  $d_{\mathbf{y}}$ :

$$\mathcal{A}Q((\bar{\Sigma}) \circ (Q^T(\mathcal{A}^*d_{\mathbf{y}})Q))Q^T + \tau_{\mathbf{y}}d_{\mathbf{y}} = -\tilde{F}_{\mathbf{y}} + \mathcal{N}_2(\mathcal{N}_4)^{-1}\tilde{F}_{\mathbf{x}}, \quad (26)$$

where  $\bar{\Sigma}$  is defined in (23). For classical SDP+ problems, the variables in AL function (4) are reduced to  $(\mathbf{y}, \mathbf{z}, \mathbf{x}, \mathbf{q})$ . In this case, the computational process is similar to (20), except that  $\bar{D}_{\mathcal{Q}}$  is zero.

## 4 Convergence analysis

In this section, we present the global, local convergence, and iteration complexity analysis of Algorithm 1.

#### 4.1 Global convergence

The proof of global convergence relies on two distinct types of descent to establish global convergence. The first is an explicit decrease in the residual norm  $\|F(\mathbf{w}^k)\|$ , directly enforced by condition (15). The second is an implicit decrease, arising from the control of the regularization parameter  $\tau_{k,i}$  under condition (16), which indirectly contributes to convergence even when the residual does not decrease immediately. Specifically, when the correction step  $\mathcal{P}_{\theta^k, l^k, \rho^k, \sigma}(\bar{\mathbf{w}}^{k,i})$  is accepted, condition (15) guarantees a measurable reduction in  $\|F(\mathbf{w}^k)\|$ . On the other hand, if the correction step is not applied, the inexact first-order step governed by (16) helps maintain  $\tau_{k,i}$  within a desirable range, thereby guiding the iterates toward optimality. We first prove in the following lemma that the sequence  $\{\|F(\mathbf{w}^k)\|\}$  generated by Algorithm 1 is bounded.

**Lemma 3** *Suppose that Assumption 1 holds. Let  $\{\mathbf{w}^k\}_{k \geq 0}$  be the iteration sequence generated by Algorithm 1. It holds that  $\|F(\mathbf{w}^k)\|$  is bounded from above. If the update (16) is conducted at the  $(k+1)$ -th iteration, the following inequality holds:*

$$\|F(\mathbf{w}^{k+1})\|^2 \leq \|F(\mathbf{w}^k)\|^2 + \frac{M}{k^{3\beta}}, \quad (27)$$

where  $M > 0$  is a constant independent of  $k$ .

**Proof** The residual mapping  $F$  defined in (8) is monotone and  $L$ -Lipschitz continuous. Define  $\bar{F} = F/L$ . The operator  $\bar{T} := I - \bar{F}$  is nonexpansive. For ease of analysis and without loss of generality, we use  $F$  and  $T$  to denote  $\bar{F}$  and  $\bar{T}$ , respectively. Note that the  $\lambda$ -averaged operator of  $T$  is  $T_\lambda := (1 - \lambda)I + \lambda T$ . Let us denote  $\hat{\mathbf{w}}^{k+1} = T_\lambda(\mathbf{w}^k) = \mathbf{w}^k - \lambda F(\mathbf{w}^k)$ . The Newton update (14) can be written as

$$\begin{aligned} \mathbf{w}^k + \mathbf{d}^{k,i} &= \mathbf{w}^k - (J^k + \tau_{k,i}I)^{-1}(F(\mathbf{w}^k) - \boldsymbol{\eta}^k) \\ &= \mathbf{w}^k - \tau_{k,i}^{-1}F(\mathbf{w}^k) + (J^k + \tau_{k,i}I)^{-1}\boldsymbol{\eta}^k + (\tau_{k,i}^{-1}I - (J^k + \tau_{k,i}I)^{-1})F(\mathbf{w}^k) \\ &= T_{\tau_{k,i}^{-1}}(\mathbf{w}^k) + (J^k + \tau_{k,i}I)^{-1}\boldsymbol{\eta}^k + (\tau_{k,i}^{-1}I - (J^k + \tau_{k,i}I)^{-1})F(\mathbf{w}^k). \end{aligned} \quad (28)$$

Define  $\mathbf{r}^k = (\tau_{k,i}^{-1}I - (J^k + \tau_{k,i}I)^{-1})F(\mathbf{w}^k)$ . It holds that

$$\begin{aligned} \|\mathbf{r}^k\| &= \|(J^k + \tau_{k,i}I)^{-1} \left( \tau_{k,i}^{-1}(J^k + \tau_{k,i}I) - I \right) F(\mathbf{w}^k)\| \\ &\leq \|(J^k + \tau_{k,i}I)^{-1} \tau_{k,i}^{-1} J^k F(\mathbf{w}^k)\| \leq \tau_{k,i}^{-2} L \|F(\mathbf{w}^k)\|. \end{aligned}$$

By using the nonexpansiveness of  $T$ , we have

$$\begin{aligned} &-2 \left\langle F(\mathbf{w}^{k+1}) - F(\mathbf{w}^k), \mathbf{w}^{k+1} - \mathbf{w}^k \right\rangle \\ &= \|T(\mathbf{w}^{k+1}) - T(\mathbf{w}^k)\|^2 - \|\mathbf{w}^{k+1} - \mathbf{w}^k\|^2 - \|F(\mathbf{w}^{k+1}) - F(\mathbf{w}^k)\|^2 \\ &\leq -\|F(\mathbf{w}^{k+1}) - F(\mathbf{w}^k)\|^2. \end{aligned} \quad (29)$$

Define  $\tilde{\eta}^k = (J_k + \tau_{k,i}I)^{-1}\eta^k$ . If  $\tau_{k,i} = \kappa_1 k^\beta$  (i.e., (15) fails) and  $k \geq 4$ , we have

$$\begin{aligned}
 \|F(\mathbf{w}^{k+1})\|^2 &= \|F(\mathbf{w}^k)\|^2 + \|F(\mathbf{w}^{k+1}) - F(\mathbf{w}^k)\|^2 + 2\langle F(\mathbf{w}^{k+1}) - F(\mathbf{w}^k), F(\mathbf{w}^k) \rangle \\
 &\stackrel{(28)}{=} \|F(\mathbf{w}^k)\|^2 + \|F(\mathbf{w}^{k+1}) - F(\mathbf{w}^k)\|^2 - 2\tau_{k,i}\langle F(\mathbf{w}^{k+1}) - F(\mathbf{w}^k), \mathbf{w}^{k+1} - \mathbf{w}^k - \mathbf{r}^k - \tilde{\eta}^k \rangle \\
 &\stackrel{(29)}{\leq} \|F(\mathbf{w}^k)\|^2 - (\tau_{k,i} - 1)\|F(\mathbf{w}^{k+1}) - F(\mathbf{w}^k)\|^2 + 2\tau_{k,i}\langle F(\mathbf{w}^{k+1}) - F(\mathbf{w}^k), \mathbf{r}^k + \tilde{\eta}^k \rangle \\
 &= \|F(\mathbf{w}^k)\|^2 - (\tau_{k,i} - 1)\|F(\mathbf{w}^{k+1}) - F(\mathbf{w}^k)\|^2 + \frac{\tau_{k,i}}{\tau_{k,i} - 1}(\mathbf{r}^k + \tilde{\eta}^k)\|^2 + \frac{\tau_{k,i}^2}{\tau_{k,i} - 1}\|\mathbf{r}^k + \tilde{\eta}^k\|^2 \\
 &\leq \|F(\mathbf{w}^k)\|^2 + \frac{2L^2}{\tau_{k,i}^3(1 - \tau_{k,i}^{-1})}\|F(\mathbf{w}^k)\|^2 + \frac{2}{\tau_{k,i} - 1}\|\eta^k\|^2 \\
 &\leq \left(1 + \frac{4\kappa_1^2 L^2}{k^{3\beta}}\right)\|F(\mathbf{w}^k)\|^2 + \frac{4\kappa_1^2 C_\eta^2}{k^{3\beta}},
 \end{aligned} \tag{30}$$

where the second inequality is due to  $\|\tilde{\eta}^k\| \leq \tau_{k,i}^{-1}\|\eta^k\|$  and the last inequality follows from  $\tau_{k,i} - 1 = \kappa_1 k^\beta - 1 \geq \frac{1}{2\kappa_1}k^\beta$ . If (15) holds, it follows that

$$\|F(\mathbf{w}^{k+1})\| \leq \nu \max_{\max(1, k-\zeta+1) \leq j \leq k} \|F(\mathbf{w}^j)\| + \varsigma_k. \tag{31}$$

We next prove the following assertion using mathematical induction: there exists a  $c > 1$  such that for  $k > 0$ ,

$$\|F(\mathbf{w}^k)\|^2 \leq c\Pi_{n=1}^k \left(1 + \frac{\tilde{L}}{n^{3\beta}}\right) \left(\|F(\mathbf{w}^0)\|^2 + \frac{1}{1 - \nu^2} \sum_{n=1}^{k-1} \varsigma_n^2 + \sum_{n=1}^k \frac{1}{n^{3\beta}}\right), \tag{32}$$

where  $\tilde{L} = 4\kappa_1^2(L^2 + C_\eta^2)$ . It is easy to verify that there exists  $c > 1$  such that (32) holds when  $k \leq 4$ . Suppose for some  $K > 4$ , and any  $k < K$  (32) holds, then in the  $K$ -th iteration, if  $\tau_{K,i} = \kappa_1 K^\beta$ , it follows from (30) and (32) that

$$\|F(\mathbf{w}^{K+1})\|^2 \leq c\Pi_{n=1}^{K+1} \left(1 + \frac{\tilde{L}}{n^{3\beta}}\right) \left(\|F(\mathbf{w}^0)\|^2 + \frac{1}{1 - \nu^2} \sum_{j=1}^{K-1} \varsigma_j^2 + \sum_{n=1}^{K+1} \frac{1}{n^{3\beta}}\right).$$

Hence (32) holds for  $\mathbf{w}^{K+1}$  if  $\tau_{K,i} = \kappa_1 K^\beta$ . For the remaining case where (15) holds, i.e.,  $\mathbf{w}^{k+1} = \tilde{\mathbf{w}}^{k,i}$ , it follows from (31) that

$$\|F(\mathbf{w}^{K+1})\| \leq \nu \sqrt{c\Pi_{n=1}^K \left(1 + \frac{\tilde{L}}{n^{3\beta}}\right) \left(\|F(\mathbf{w}^0)\|^2 + \frac{1}{1 - \nu^2} \sum_{j=1}^{K-1} \varsigma_j^2 + \sum_{n=1}^K \frac{1}{n^{3\beta}}\right)} + \varsigma_K.$$

According to the AM-GM inequality, i.e.,  $(a + b)^2 \leq (1 + \rho)a^2 + (1 + 1/\rho)b^2$  with  $\rho = \frac{1-\nu^2}{\nu^2}$  for all  $a, b \in \mathbb{R}$  and  $\rho > 0$ , we have

$$\|F(\mathbf{w}^{K+1})\|^2 \leq c\Pi_{n=1}^K \left(1 + \frac{\tilde{L}}{n^{3\beta}}\right) \left(\|F(\mathbf{w}^0)\|^2 + \frac{1}{1 - \nu^2} \sum_{j=1}^{K-1} \varsigma_j^2 + \sum_{n=1}^K \frac{1}{n^{3\beta}}\right) + \frac{1}{1 - \nu^2} \varsigma_K^2,$$

Hence, (32) holds. Since  $\prod_{k=1}^{\infty} \left(1 + \frac{\tilde{L}^2}{k^{3\beta}}\right) < \exp(\sum_{k=1}^{\infty} \frac{\tilde{L}^2}{k^{3\beta}}) < \infty$  and  $\sum_{j=1}^{\infty} \varsigma_j^2$  is finite, we can conclude that  $\|F(\mathbf{w}^k)\|$  is bounded. Let  $M_1 > 0$  be the constant such that for all  $k$ ,  $\|F(\mathbf{w}^k)\|^2 \leq M_1$ . If  $\tau_{k,i} = \kappa_1 k^\beta$ , it holds that

$$\|F(\mathbf{w}^{k+1})\|^2 \leq \|F(\mathbf{w}^k)\|^2 + \frac{M}{k^{3\beta}},$$

where  $M = 4L^2 M_1 \kappa_1^2 + 4\kappa_1^2 C_\eta^2$ . ■

Next, we establish the global convergence of Algorithm 1. This is demonstrated by showing that the residual norm converges to zero.

**Theorem 4** *Suppose that Assumption 1 holds. Let  $\{\mathbf{w}^k\}$  be the sequence generated by Algorithm 1. The residual  $F(\mathbf{w}^k)$  converges to 0, i.e.,*

$$\lim_{k \rightarrow \infty} F(\mathbf{w}^k) = 0. \quad (33)$$

**Proof** Let us consider the following three cases, i.e., (i) the total number of steps involving (15) is finite, (ii) the total number of steps involving (16) is finite, (iii) steps associated with both (15) and (16) are encountered infinitely many times. Specifically, if (i) happens, according to the update of  $\mathbf{w}^{k+1}$  (28), we have

$$\begin{aligned} \|\mathbf{w}^{k+1} - \mathbf{w}_*\| &\leq (1 - \tau_{k,i}^{-1})\|\mathbf{w}^k - \mathbf{w}_*\| + \tau_{k,i}^{-1}\|T(\mathbf{w}^k) - \mathbf{w}_*\| + \tau_{k,i}^{-1}\|\mathbf{e}^k\| \\ &\leq \|\mathbf{w}^k - \mathbf{w}_*\| + \tau_{k,i}^{-1}\|\mathbf{e}^k\|, \end{aligned}$$

where  $\mathbf{e}^k = \tau_{k,i}(\mathbf{r}^k + \tilde{\eta}^k)$ . Since  $\tau_{k,i}^{-1}\|\mathbf{e}^k\|$  is summable, it follows that  $\|\mathbf{w}^{k+1} - \mathbf{w}_*\|^2$  is bounded. In this case, for every  $\mathbf{w}_* \in \mathbf{W}_*$ , we have

$$\begin{aligned} \|\mathbf{w}^{k+1} - \mathbf{w}_*\|^2 &= \|(1 - \tau_{k,i}^{-1})(\mathbf{w}^k - \mathbf{w}_*) + \tau_{k,i}^{-1}(T(\mathbf{w}^k) - \mathbf{w}_* + \mathbf{e}^k)\|^2 \\ &= (1 - \tau_{k,i}^{-1})\|\mathbf{w}^k - \mathbf{w}_*\|^2 - \tau_{k,i}^{-1}(1 - \tau_{k,i}^{-1})(\|F(\mathbf{w})\|^2 + 2\langle F(\mathbf{w}), \mathbf{e}^k \rangle + \|\mathbf{e}^k\|^2) \\ &\quad + \tau_{k,i}^{-1}(\|T(\mathbf{w}^k) - \mathbf{w}_*\|^2 + 2\langle T(\mathbf{w}^k) - \mathbf{w}_*, \mathbf{e}^k \rangle + \|\mathbf{e}^k\|^2) \\ &\leq \|\mathbf{w}^k - \mathbf{w}_*\|^2 - \tau_{k,i}^{-1}(1 - \tau_{k,i}^{-1})\|F(\mathbf{w}^k)\|^2 + \underbrace{2\tau_{k,i}^{-1}\langle \mathbf{w}^k - \mathbf{w}_*, \mathbf{e}^k \rangle + (\tau_{k,i}^{-2})\|\mathbf{e}^k\|^2}_{:=\xi^k} \\ &\leq \|\mathbf{w}^k - \mathbf{w}_*\|^2 - \tau_{k,i}^{-1}(1 - \tau_{k,i}^{-1})\|F(\mathbf{w}^k)\|^2 + 2\tau_{k,i}^{-1}\|\mathbf{w}^k - \mathbf{w}_*\|\|\mathbf{e}^k\| + \tau_{k,i}^{-2}\|\mathbf{e}^k\|^2, \end{aligned}$$

where the second equality follows from  $\|\tau_{k,i}^{-1}a + (1 - \tau_{k,i}^{-1})b\|^2 = \tau_{k,i}^{-1}\|a\|^2 + (1 - \tau_{k,i})\|b\|^2 + \tau_{k,i}(1 - \tau_{k,i})\|a + b\|^2$  for any  $a, b \in \mathbb{R}^n$ . Since  $\|\mathbf{w}^k - \mathbf{w}_*\|$  is bounded, it follows that  $\|\xi^k\|^2$  is summable and hence we have

$$\sum_{i=0}^{\infty} \tau_{k,i}^{-1}\|F(\mathbf{w}^i)\|^2 \leq \|\mathbf{w}^0 - \mathbf{w}_*\|^2 + \sum_{i=0}^{\infty} \|\xi^i\|^2. \quad (34)$$

Given that  $\tau_{k,i} = \kappa_1 k^\beta$  and  $\beta \in (\frac{1}{3}, 1)$ , there exists a constant  $C_F$  such that  $\|F(\mathbf{w}^k)\|^2 \leq C_F k^{-\frac{2}{3}}$ . Hence it follows that (33) holds. We next consider the case (ii) where there exists

a  $K_0 > 0$  such that  $\|F(\mathbf{w}^{k+1})\| \leq \nu \max_{\max(1, k-\zeta+1) \leq j \leq k} \|F(\mathbf{w}^j)\| + \varsigma_k$  for  $k \geq K_0$ . It follows from (Armand and Omheni, 2017, Lemma 3.2) that (33) holds. In terms of (iii), let  $k_1, k_2, \dots$  be the indices corresponding to the steps where (15) hold. According to Lemma 3, we have for any  $k_n + 1 < j \leq k_{n+1}$ ,

$$\|F(\mathbf{w}^{j+1})\|^2 \leq \|F(\mathbf{w}^j)\|^2 + \frac{M}{j^{3\beta}} \leq \|F(\mathbf{w}^{k_n+1})\|^2 + \sum_{k=k_n}^j \frac{M}{k^{3\beta}}. \quad (35)$$

Let  $a_n = \max_{\max(1, n-\zeta+1) \leq j \leq n} \|F(\mathbf{w}^{k_j+1})\|$  and  $\pi_n := \sqrt{\sum_{k=k_n+1}^{k_{n+1}-1} \frac{M}{k^{3\beta}}}$ . Due to  $k_{n+\zeta} - k_n \geq \zeta$ , we have the recursion

$$\|F(\mathbf{w}^{k_{n+1}+1})\| \leq \nu a_n + \nu \max_{\max(1, n-\zeta+1) \leq j \leq n} (\pi_j + \varsigma_{k_j}). \quad (36)$$

Denote  $c_n := a_n \zeta$ . Inequality (36) gives

$$c_{n+1} \leq \nu c_n + \nu \sum_{l=n\zeta}^{(n+1)\zeta-1} \max_{\max(1, l-\zeta+1) \leq j \leq l} (\pi_j + \varsigma_{k_j}). \quad (37)$$

It follows from (Xu et al., 2015, Lemma 2) that there exist constants  $C_1 > 0$  and  $C_2 > 0$  such that

$$\sum_{n=0}^{\infty} \|c_{n+1}\|^2 \leq C_1 \sum_{n=0}^{\infty} \left[ \sum_{l=n\zeta}^{(n+1)\zeta-1} \max_{\max(1, l-\zeta+1) \leq j \leq l} (\pi_j + \varsigma_{k_j}) \right]^2 + C_2. \quad (38)$$

Note that for sufficiently large  $n \geq N$ ,

$$\begin{aligned} & \left[ \sum_{l=n\zeta}^{(n+1)\zeta-1} \max_{\max(1, l-\zeta+1) \leq j \leq l} \pi_j + \varsigma_{k_j} \right]^2 \leq \left( \sum_{l=n\zeta}^{(n+1)\zeta-1} \sum_{j=l-\zeta+1}^l \pi_j + \varsigma_{k_j} \right)^2 \\ & \leq \left( \zeta \sum_{l=(n-1)\zeta+1}^{(n+1)\zeta} (\pi_l + \varsigma_{k_l}) \right)^2 \leq 4\zeta^2 \sum_{k=k_{(n-1)\zeta+1}}^{k_{(n+1)\zeta}} \left( \frac{M}{k^{3\beta}} + \varsigma_k^2 \right). \end{aligned}$$

This implies

$$\sum_{n=N}^{\infty} \left[ \sum_{l=n\zeta}^{(n+1)\zeta-1} \max_{\max(1, l-\zeta+1) \leq j \leq l} \pi_j + \varsigma_n \right]^2 \leq 8\zeta^3 \sum_{n=k_{(N-1)\zeta}}^{\infty} \left( \frac{M}{n^{3\beta}} + \varsigma_n^2 \right) < \infty$$

and  $\lim_{n \rightarrow \infty} \|c_n\| = 0$ . Furthermore, by the definition of  $c_n$  and the summability of  $\{\varsigma_k^2\}_{k=1}^{\infty}$ , we have  $\lim_{j \rightarrow \infty} \|F(\mathbf{w}^{k_j+1})\| \rightarrow 0$ . Using (35) and  $\beta > \frac{1}{3}$ , (33) holds.  $\blacksquare$

The above proof combines the explicit descent in (15) with the implicit descent in (16) derived from the inexact first-order step. Since the correction step  $\mathcal{P}_{\theta^k, l^k, \rho^k, \sigma}(\bar{\mathbf{w}}^{k,i})$  is accepted only when (15) holds, the above analysis of global convergence is independent of the projection.

## 4.2 Local convergence

The goal in this section is to establish the superlinear convergence of Algorithm 1, which is proved in (Hu et al., 2025) under the SC condition. However, since the SC condition may not hold in general, we aim to extend the desired result with the correction step without assuming SC. The proof outline is listed below. First, we show the manifold identification of the iterates empowered by the correction step. Then, under the smoothness of  $F$  on the manifold, the local superlinear convergence for  $\{\mathbf{w}^k\}$  holds under the local error bound condition. We introduce the notion of partial smoothness (Lewis et al., 2022) in the following.

**Definition 5** ( $C^p$ -partial smoothness) *Consider a proper closed function  $\phi : \mathbb{R}^n \rightarrow \bar{\mathbb{R}}$  and a  $C^p$  ( $p \geq 2$ ) embedded submanifold  $\mathcal{M}$  of  $\mathbb{R}^n$ . The function  $\phi$  is said to be  $C^p$ -partly smooth at  $x \in \mathcal{M}$  for  $v \in \partial\phi(x)$  relative to  $\mathcal{M}$  if*

- (i) *Smoothness:  $\phi$  restricted to  $\mathcal{M}$  is  $C^p$ -smooth near  $x$ .*
- (ii) *Prox-regularity:  $\phi$  is prox-regular at  $x$  for  $v$ .*
- (iii) *Sharpness:  $\text{par } \partial_p \phi(x) = N_{\mathcal{M}}(x)$ , where  $\partial_p \phi(x)$  denotes the set of proximal subgradients of  $\phi$  at point  $x$ ,  $\text{par } \Omega$  is the subspace parallel to  $\Omega$  and  $N_{\mathcal{M}}(x)$  is the normal space of  $\mathcal{M}$  at  $x$ .*
- (iv) *Continuity: There exists a neighborhood  $V$  of  $v$  such that the set-valued mapping  $V \cap \partial\phi$  is inner semicontinuous at  $x$  relative to  $\mathcal{M}$ .*

Since  $h$  is an elementwise indicator function on a polyhedral convex set, we can check that  $h, \delta_{\mathcal{Q}}$ , and  $\delta_{\mathcal{K}}$  are partly smooth (Lewis, 2002). One usage of partial smoothness is connecting the relative interior condition in (iii) with SC to derive certain smoothness in nonsmooth optimization (Bareilles et al., 2023). In addition to the partial smoothness, the local error bound condition (Yue et al., 2019) is a powerful tool for analyzing convergence in the absence of nonsingularity.

**Definition 6** *We say the local error bound condition holds if there exist  $\gamma_l > 0$  and  $\varepsilon > 0$  such that for all  $\mathbf{w}$  with  $\text{dist}(\mathbf{w}, \mathbf{W}_*) \leq \varepsilon$ , it holds that*

$$\|F(\mathbf{w})\| \geq \gamma_l \text{dist}(\mathbf{w}, \mathbf{W}_*), \quad (39)$$

where  $\mathbf{W}_*$  is the solution set of  $F(\mathbf{w}) = 0$  and  $\text{dist}(\mathbf{w}, \mathbf{W}_*) := \arg \min_{\mathbf{u} \in \mathbf{W}_*} \|\mathbf{w} - \mathbf{u}\|$ .

We next present some notations. For any solution  $\mathbf{w}_* \in \mathbf{W}_*$ , let  $\lambda^* \in \mathbb{R}^n$  be the eigenvalues of  $\sigma(\mathcal{A}^*(\mathbf{y}_*) + \mathbf{z}_* - \mathbf{c}) + \mathbf{x}_*$ . We denote the threshold values with respect to  $\mathbf{w}_*$  as

$$\begin{aligned} \bar{\theta} &:= \min(\lambda_{\alpha_1}^*, |\lambda_{\alpha_2}^*|), \\ \bar{l} &:= \min_{i \in I_{\mathcal{Q}}} \{\text{dist}(-(\mathbf{y}_*)_i, \text{bd}(\mathcal{N}_{\mathcal{Q}_i}((\mathbf{u}_*)_i)))\}, \\ \bar{\rho} &:= \min_{(i,j) \in I_h} \{\text{dist}(-(\mathbf{z}_*)_{i,j}, \text{bd}(\partial h_{i,j}((\mathbf{x}_*)_{i,j})))\}, \end{aligned} \quad (40)$$

where  $\alpha_1 := \{i | \lambda_i^* > 0\}$ ,  $\alpha_2 := \{i | \lambda_i^* < 0\}$ ,  $I_{\mathcal{Q}} := \{i | -(\mathbf{y}_*)_i \in \text{ri}(\partial \mathcal{N}_{\mathcal{Q}_i}((\mathbf{u}_*)_i))\}$ ,  $I_h := \{(i,j) | -(\mathbf{z}_*)_{i,j} \in \text{ri}(\partial h_{i,j}((\mathbf{x}_*)_{i,j}))\}$ , and  $h_{i,j}$  denotes the function  $h$  restricted to index  $(i,j)$ .



According to (Rockafellar and Wets, 2009, Page 64, Exercise 2.11), the relative interior and interior coincide in the case of  $\mathbb{R}$ . Hence it follows from the definition of  $\alpha_1, \alpha_2, I_Q, I_h$  that  $\bar{\theta}, \bar{l}$ , and  $\bar{\rho}$  are well defined.

Firstly, we show by the assumptions on  $h, Q$  and  $\mathcal{K}$  that there exists a manifold defined with respect to each solution  $\mathbf{w}_* \in \mathbf{W}_*$ , and such manifold will be useful in the analysis of local smoothness of  $F$ .

**Lemma 7** *For given  $\sigma$  and  $\mathbf{w}_* \in \mathbf{W}_*$ , we define the following sets:*

$$\begin{aligned}\overline{\mathcal{M}}_{\mathbf{w}_*, I_h} &:= \{\mathbf{w} | (\mathbf{q} - \sigma \mathbf{z})_{i,j} = (\mathbf{q}_* - \sigma \mathbf{z}_*)_{i,j} \text{ for } (i,j) \notin I_h\}, \\ \overline{\mathcal{M}}_{\mathbf{w}_*, I_Q} &:= \{\mathbf{w} | (\mathbf{u} - \sigma \mathbf{y})_i = (\mathbf{u}_* - \sigma \mathbf{y}_*)_i \text{ for } i \notin I_Q\}, \\ \overline{\mathcal{M}}_{\mathbf{w}_*, r_{\mathcal{K}}} &:= \{\mathbf{w} | \text{rank}(\mathbf{x} - \sigma(\mathcal{A}^*(\mathbf{y}) - \mathbf{c} + \mathbf{z})) = |\alpha_1| + |\alpha_2|\}.\end{aligned}\tag{41}$$

Then  $\overline{\mathcal{M}}_{\mathbf{w}_*} := \overline{\mathcal{M}}_{\mathbf{w}_*, I_h} \cap \overline{\mathcal{M}}_{\mathbf{w}_*, I_Q} \cap \overline{\mathcal{M}}_{\mathbf{w}_*, r_{\mathcal{K}}}$  is a manifold.

**Proof** Without loss of generality, for  $\mathbf{w} \in \overline{\mathcal{M}}_{\mathbf{w}_*, r_{\mathcal{K}}}$ , we assume that the  $r \times r$  matrix in the upper left corner of  $\mathbf{x} - \sigma(\mathcal{A}^*(\mathbf{y}) - \mathbf{c} + \mathbf{z})$  is invertible. For any  $\mathbf{r} = \begin{bmatrix} \mathbf{r}_{11} & \mathbf{r}_{12} \\ \mathbf{r}_{21} & \mathbf{r}_{22} \end{bmatrix} \in \mathbb{R}^{n \times n}$ , where  $\mathbf{r}_{11} \in \mathbb{R}^{r \times r}$  be invertible and  $\mathbf{r}_{22} \in \mathbb{R}^{(n-r) \times (n-r)}$ , define  $f : \mathbf{x} \in \mathbb{R}^{n \times n} \rightarrow \mathbf{x}_{22} - \mathbf{x}_{21} \mathbf{x}_{11}^{-1} \mathbf{x}_{12} \in \mathbb{R}^{(n-r) \times (n-r)}$ , and  $g : \mathbf{w} \in \mathbb{R}^{4n \times n+m} \rightarrow \mathbf{x} - \sigma(\mathcal{A}^*(\mathbf{y}) - \mathbf{c} + \mathbf{z}) \in \mathbb{R}^{n \times n}$ . Then, for every  $\mathbf{w} \in \overline{\mathcal{M}}_{\mathbf{w}_*, r_{\mathcal{K}}}$ , it follows that  $\psi(\mathbf{w}) = 0$ , where  $\psi := f \circ g$ . If the  $r \times r$  matrix in the upper left corner of  $\mathbf{x} - \sigma(\mathcal{A}^*(\mathbf{y}) - \mathbf{c} + \mathbf{z})$  is not invertible, we can construct another local defining function using the same procedure (Boumal, 2023, Section 7.5). For  $g_Q(\mathbf{w}) := ((\mathbf{u} - \sigma \mathbf{y}) - (\mathbf{u}_* - \sigma \mathbf{y}_*))_{I_Q^c}$ ,  $g_h(\mathbf{w}) := ((\mathbf{q} - \sigma \mathbf{z}) - (\mathbf{q}_* - \sigma \mathbf{z}_*))_{I_h^c}$ , we define

$$\bar{\psi} := \begin{bmatrix} \psi \\ g_Q \\ g_h \end{bmatrix} : \mathbb{R}^{4n \times n+m} \rightarrow \mathbb{R}^{(n-r) \times (n-r) + |I_Q^c| + |I_h^c|}.\tag{42}$$

We now prove that the Jacobian matrix of  $\bar{\psi}$  is full rank. According to (Boumal, 2023, Section 7.5), for given  $\mathbf{r} \in \mathbb{R}^{n \times n}$ ,  $\mathbf{w} \in \mathbb{R}^{4n \times n+m}$  and any  $\mathbf{g} \in \mathbb{R}^{n \times n}$ ,  $\mathbf{o}_1 \in \mathbb{R}^m$ ,  $\mathbf{o}_2, \mathbf{o}_3, \mathbf{o}_4, \mathbf{o}_5 \in \mathbb{R}^{n \times n}$ ,  $\mathbf{o} = [\mathbf{o}_1, \mathbf{o}_2, \mathbf{o}_3, \mathbf{o}_4, \mathbf{o}_5] \in \mathbb{R}^{4n \times n+m}$ , it follows that

$$\begin{aligned}Df(\mathbf{r})[\mathbf{g}] &= \mathbf{g}_{22} - \mathbf{g}_{21} \mathbf{r}_{11}^{-1} \mathbf{r}_{12} + \mathbf{r}_{21} \mathbf{r}_{11}^{-1} \mathbf{g}_{11} \mathbf{r}_{11}^{-1} \mathbf{r}_{21} - \mathbf{r}_{21} \mathbf{r}_{11}^{-1} \mathbf{g}_{12}, \\ Dg(\mathbf{w})[\mathbf{o}] &= -\sigma \mathcal{A}^* \mathbf{o}_1 - \sigma \mathbf{o}_2 + \mathbf{o}_3, \\ Dg_Q(\mathbf{w})[\mathbf{o}] &= (\mathbf{o}_4 - \sigma \mathbf{o}_1)_{I_Q^c}, \\ Dg_h(\mathbf{w})[\mathbf{o}] &= (\mathbf{o}_5 - \sigma \mathbf{o}_2)_{I_h^c}.\end{aligned}\tag{43}$$

Consequently, for any  $(\bar{\mathbf{a}}, \bar{\mathbf{b}}, \bar{\mathbf{c}}) \in \mathbb{R}^{(n-r) \times (n-r) + |I_Q^c| + |I_h^c|}$  with  $\bar{\mathbf{a}} \in \mathbb{R}^{(n-r) \times (n-r)}$ ,  $\bar{\mathbf{b}} \in \mathbb{R}^{|I_Q^c|}$ ,  $\bar{\mathbf{c}} \in \mathbb{R}^{|I_h^c|}$ , set  $\mathbf{o} = (0, 0, \mathbf{a}, \mathbf{b}, \mathbf{c})$ , where  $\mathbf{a} = \begin{bmatrix} 0 & 0 \\ 0 & \bar{\mathbf{a}} \end{bmatrix} \in \mathbb{R}^{n \times n}$ ,  $(\mathbf{b})_{I_Q^c} = \bar{\mathbf{b}}$ , and  $(\mathbf{c})_{I_h^c} = \bar{\mathbf{c}}$ . It follows from the definition of  $\bar{\psi}$  that  $D\bar{\psi}[\mathbf{o}] = (\bar{\mathbf{a}}, \bar{\mathbf{b}}, \bar{\mathbf{c}})$ , which indicates that  $D\bar{\psi}$  is full rank. Consequently,  $\bar{\psi}(\mathbf{w}) = 0$  defines a manifold locally and we complete the proof.  $\blacksquare$

We then make the following assumptions.

**Assumption 2** Let  $\{\mathbf{w}^k\}$  be the iterate sequence generated by Algorithm 1.

(A1) The local error bound condition (39) holds.

(A2) The sequence  $\{\boldsymbol{\eta}^k\}$  satisfies  $\|\boldsymbol{\eta}^k\| \leq c_\eta \|F(\mathbf{w}^k)\|^q$ , where  $q \in (1, 2]$ .

(A3) For a solution  $\mathbf{w}_* \in \mathbf{W}_*$ , the correction parameters satisfy  $\theta^k \in (0, \bar{\theta})$ ,  $l^k \in (0, \bar{l})$ , and  $\rho^k \in (0, \bar{\rho})$ , where  $\bar{\theta}$ ,  $\bar{l}$ , and  $\bar{\rho}$  are defined in (40) with respect to  $\mathbf{w}_*$ .

**Remark 8** The Assumptions (A1), and (A2) are commonly used assumptions in local convergence analysis (Hu et al., 2025; Bareilles et al., 2023; Yue et al., 2019). As shown in Ding and Udell (2023, Corollary 1), a variant of the local error bound condition holds under strong duality and dual strict complementarity. Furthermore, Assumption (A1) is much weaker than the BD-regularity condition adopted in (Xiao et al., 2018b) and (Li et al., 2018). We also conduct some numerical verifications of (A1) in Section 5.2. Assumption (A2) specifies the solution accuracy of the Newton equation, which is readily satisfied in numerical experiments. Assumption (A3) is assumed with respect to a solution  $\mathbf{w}_* \in \mathbf{W}_*$ . It is used to ensure the manifold identification of the iterations and desired smoothness of  $F$ . We note that Assumption (A3) is designed for the general problem (1) and can be simplified for concrete examples. Particularly, for SDP, since there is no  $h$  and  $\mathcal{Q}$ , the Assumption (A3) reduces to  $\theta \in (0, \bar{\theta})$ . A similar condition has also been assumed in (Feng et al., 2025, Theorem 2). However, our approach to defining these parameters and the correction step differs substantially. Specifically, we identify a smooth manifold on which the iterates eventually lie and establish superlinear convergence without requiring any nonsingular element in the generalized Jacobian of  $F$ , unlike (Feng et al., 2025). This indicates the applicability of our superlinear convergence to nonisolated minima, while their result does not cover it. Furthermore, if SC holds, it follows that  $F$  is locally smooth on the whole space (Hu et al., 2025, Lemma 2). Hence no correction step is needed.

For a solution  $\mathbf{w}_* \in \mathbf{W}_*$ , let  $\mathcal{M}_{\mathbf{w}_*, h}$ ,  $\mathcal{M}_{\mathbf{w}_*, \mathcal{Q}}$ , and  $\mathcal{M}_{\mathbf{w}_*, \mathcal{K}}$  be the associated smooth manifolds of the partly smooth functions  $h, \delta_{\mathcal{Q}}, \delta_{\mathcal{K}}$ . It follows from the definition of partial smoothness and  $\mathbf{q}_* = \mathbf{x}_*$  that  $\mathbf{q}_* \in \mathcal{M}_{\mathbf{w}_*, h}$ ,  $\mathbf{u}_* \in \mathcal{M}_{\mathbf{w}_*, \mathcal{Q}}$ ,  $\mathbf{x}_* \in \mathcal{M}_{\mathbf{w}_*, \mathcal{K}}$ . Based on the construction of correction step, we have the following local smoothness result.

**Lemma 9** For a solution  $\mathbf{w}_* \in \mathbf{W}_*$ , there exists a neighborhood  $V$  of  $\mathbf{w}_*$  such that  $F(\mathbf{w})$  is locally smooth on  $V \cap \overline{\mathcal{M}}_{\mathbf{w}_*}$ .

**Proof** Since  $h, \delta_{\mathcal{Q}}$ , and  $\delta_{\mathcal{K}}$  are proper closed and convex functions, according to (Beck, 2017, Theorem 6.3, 6.4, 6.42),  $\text{prox}_{\sigma h}(\mathbf{x} - \sigma \mathbf{z})$ ,  $\Pi_{\mathcal{Q}}(\mathbf{u} - \sigma \mathbf{y})$ ,  $\Pi_{\mathcal{K}}(\mathbf{x} - \sigma(\mathcal{A}^*(\mathbf{y}) - \mathbf{c} + \mathbf{z}))$  are monotone, single-valued, and Lipschitz. Define  $h_{I_h}$  be the function when restricted on  $I_h$ , then we can conclude that there exists a neighborhood  $V_1$  of  $\mathbf{w}_*$  such that  $\text{prox}_{\sigma h_{I_h}}(\mathbf{q} - \sigma \mathbf{z}) \in \mathcal{M}_{\mathbf{w}_*, h}$  for  $\mathbf{w} \in V_1 \cap \overline{\mathcal{M}}_{\mathbf{w}_*, I_h}$  by (Drusvyatskiy and Lewis, 2014, Proposition 10.12). According to the definition of  $\overline{\mathcal{M}}_{\mathbf{w}_*, I_h}$ ,  $\text{prox}_{\sigma h}(\mathbf{q} - \sigma \mathbf{z}) \in \mathcal{M}_{\mathbf{w}_*, h}$  for all  $\mathbf{w} \in V_1 \cap \overline{\mathcal{M}}_{\mathbf{w}_*, I_h}$ . The result that there exists  $V_2$  such that  $\Pi_{\mathcal{Q}}(\mathbf{u} - \sigma \mathbf{y}) \in \mathcal{M}_{\mathbf{w}_*, \mathcal{Q}}$  for  $\mathbf{w} \in \overline{\mathcal{M}}_{\mathbf{w}_*, I_{\mathcal{Q}}} \cap V_2$  can be proved analogously. Since  $\text{rank}(\mathbf{x}_* - \sigma(\mathcal{A}^*(\mathbf{y}_*) - \mathbf{c} + \mathbf{z}_*)) = |\alpha_1| + |\alpha_2|$  and  $\text{rank}(\mathbf{x}_*) = |\alpha_1|$ , there exists a neighborhood  $V_3$  of  $\mathbf{w}_*$  such that the number of its positive eigenvalues is  $|\alpha_1|$  and the number of negative eigenvalues is  $|\alpha_2|$  when  $\mathbf{w}$  is restricted on  $V_3 \cap \overline{\mathcal{M}}_{\mathbf{w}_*, r_{\mathcal{K}}}$ . As a consequence, we have

$$\Pi_{\mathcal{K}}(\mathbf{x} - \sigma(\mathcal{A}^*(\mathbf{y}) - \mathbf{c} + \mathbf{z})) \in \mathcal{M}_{\mathbf{w}_*, \mathcal{K}} \text{ for all } \mathbf{w} \in V_3 \cap \overline{\mathcal{M}}_{\mathbf{w}_*, r_{\mathcal{K}}}.$$

Combining the partial smoothness of  $h, \delta_Q$ , and  $\delta_K$ , and according to a similar scheme in (Hu et al., 2025, Lemma 2), (Lewis and Malick, 2008, Lemma 2.1), we have that  $\text{prox}_{\sigma h_1}(\mathbf{w}) := \text{prox}_{\sigma h}(\mathbf{q} - \sigma \mathbf{z})$ ,  $\text{prox}_{\sigma h_2}(\mathbf{w}) := \Pi_Q(\mathbf{u} - \sigma \mathbf{y})$ , and  $\text{prox}_{\sigma h_3}(\mathbf{w}) := \Pi_K(\mathbf{x} - \sigma(\mathcal{A}^*(\mathbf{y}) - \mathbf{c} + \mathbf{z}))$  are locally smooth around  $\mathbf{w}_*$  on  $\overline{\mathcal{M}}_{\mathbf{w}_*, I_h}$ ,  $\overline{\mathcal{M}}_{\mathbf{w}_*, I_Q}$ , and  $\overline{\mathcal{M}}_{\mathbf{w}_*, r_K}$ , respectively. According to the definition of  $F$  and let  $V = V_1 \cap V_2 \cap V_3$ , the proof is completed.  $\blacksquare$

The above result significantly differs from the existing manifold identification results in (Bareilles et al., 2023; Deng et al., 2025; Liang et al., 2017) where SC is necessary. As noted in (Liang et al., 2017, Remark 3.5), relaxing SC is a challenging problem. We next prove that  $\{\mathbf{w}^k\}$  generated by Algorithm 1 stays on the smooth manifold through the correction step  $\mathcal{P}_{\theta, l, \rho, \sigma}$ . Furthermore, under the local smoothness condition, (15) happens all the time and  $\tau_{k,i}$  does not need to satisfy (16). Hence, the transition to the local superlinear convergence for  $\{\mathbf{w}^k\}$  holds.

**Theorem 10** *Let Assumptions 1, (A1), and (A2) hold. For sequence  $\{\mathbf{w}^k\}$  generated by Algorithm 1, if there exist a solution  $\hat{\mathbf{w}}_* \in \Pi_{\mathbf{W}_*}(\mathbf{w}^K)$  and a constant  $\delta_{\hat{\mathbf{w}}_*}$  for some  $\mathbf{w}^K \in B(\hat{\mathbf{w}}_*, \delta_{\hat{\mathbf{w}}_*}) \cap \overline{\mathcal{M}}_{\hat{\mathbf{w}}_*}$ , (A3) holds for  $\hat{\mathbf{w}}_*$ , the following conclusions hold.*

(C1) *Condition (15) always holds with  $i = 0$  for  $k > K$  and  $\mathbf{w}^k$  lies in the manifold  $\overline{\mathcal{M}}_{\hat{\mathbf{w}}_*}$ .*

(C2) *The generated sequence  $\{\mathbf{w}^k\}$  converges to some solution  $\mathbf{w}_* \in \overline{\mathcal{M}}_{\hat{\mathbf{w}}_*}$  superlinearly.*

**Proof** (C1): By Lemma 7, we conclude that  $F$  is locally smooth on  $\overline{\mathcal{M}}_{\hat{\mathbf{w}}_*}$ . Hence the local quadratic upper bound of  $F$ , i.e., condition (Hu et al., 2025, Assumption 3(A1)), holds. For  $i = 0$  (ignoring the subscript  $i$ ), let  $\bar{\mathbf{w}}^K$  be defined in (14),  $\bar{\lambda}^K$  be the eigenvalue of  $\bar{\mathbf{x}}^K + \sigma(\mathcal{A}^*(\bar{\mathbf{y}}^K) + \bar{\mathbf{z}}^K - \mathbf{c})$ , and  $\hat{\lambda}^*$  be the eigenvalue of  $\hat{\mathbf{x}}_* + \sigma(\mathcal{A}^*(\hat{\mathbf{y}}_*) + \hat{\mathbf{z}}_* - \mathbf{c})$ . It follows from (Hu et al., 2025, Lemma 5) that there exists  $\bar{c}$  such that  $\|\mathbf{d}^K\| \leq \bar{c}(\text{dist}(\mathbf{w}^K, \mathbf{W}_*) + \|\boldsymbol{\eta}^K\|)$ . Hence there exists  $\delta_{\hat{\mathbf{w}}_*, 1}$  such that for  $\mathbf{w}^K \in B(\hat{\mathbf{w}}_*, \delta_{\hat{\mathbf{w}}_*, 1})$ , we have  $\|\bar{\lambda}^K - \hat{\lambda}^*\|_\infty < \frac{\bar{\theta}}{2}$ . Consequently,  $|\bar{\lambda}_{\alpha_1 \cup \alpha_2}^K| > \frac{\bar{\theta}}{2}$  and  $|\bar{\theta}_{(\alpha_1 \cup \alpha_2)^c}^K| < \frac{\bar{\theta}}{2}$ . Then according to the definition of  $\mathcal{P}_{\theta, l, \rho, \sigma}$ ,  $\tilde{\mathbf{w}}^K$  and (A3) in Assumption 2,  $\text{rank}(\sigma(\mathcal{A}^*(\tilde{\mathbf{y}}^K) - \mathbf{c}) + \tilde{\mathbf{x}}^K) = |\alpha_1| + |\alpha_2|$ . Analogously, for the index where SC does not hold, it holds that  $(\hat{\mathbf{u}}_*)_i \in \text{bd}(\mathcal{Q}_i)$  and  $\hat{\mathbf{y}}_{*, i} \in -\text{bd}(\mathcal{N}_{\mathcal{Q}_i}(\hat{\mathbf{u}}_{*, i}))$ . As a consequence, it holds that there exist  $\delta_{\hat{\mathbf{w}}_*, 2}, \delta_{\hat{\mathbf{w}}_*, 3}$  such that  $(\tilde{\mathbf{u}}^K - \sigma \tilde{\mathbf{y}}^K)_i = (\hat{\mathbf{u}}_* - \sigma \hat{\mathbf{y}}_*)_i$ ,  $i \notin I_Q$  and  $(\tilde{\mathbf{q}}^K - \sigma \tilde{\mathbf{z}}^K)_{i,j} = (\hat{\mathbf{q}}_* - \sigma \hat{\mathbf{z}}_*)_{i,j}$ ,  $(i, j) \notin I_h$  for  $\mathbf{w}^K \in B(\hat{\mathbf{w}}_*, \delta_{\hat{\mathbf{w}}_*, 2})$  and  $\mathbf{w}^K \in B(\hat{\mathbf{w}}_*, \delta_{\hat{\mathbf{w}}_*, 3})$ , respectively. Hence  $\mathcal{P}_{\theta K, lK, \rho K, \sigma}(\mathbf{w}^K + \mathbf{d}^K) \in \overline{\mathcal{M}}_{\hat{\mathbf{w}}_*}$  holds.

Since (A1) and (A2) in Assumption 2 hold and  $\tilde{\mathbf{w}}^K = \mathcal{P}_{\theta K, lK, \rho K, \sigma}(\mathbf{w}^K + \mathbf{d}^K) \in \overline{\mathcal{M}}_{\hat{\mathbf{w}}_*}$ , it follows from (Hu et al., 2025, Lemma 6) that there exists  $\delta_{\hat{\mathbf{w}}_*, 4}$  such that for  $\mathbf{w}^K \in B(\hat{\mathbf{w}}_*, \delta_{\hat{\mathbf{w}}_*, 4})$ , we have:

$$\text{dist}(\mathcal{P}_{\theta K, lK, \rho K, \sigma}(\mathbf{w}^K + \mathbf{d}^K), \mathbf{W}_*) \leq \gamma_l^{-1} \|F(\mathcal{P}_{\theta K, lK, \rho K, \sigma}(\mathbf{w}^K + \mathbf{d}^K))\| \leq c_2 \text{dist}(\mathbf{w}^K, \mathbf{W}_*)^q, \quad (44)$$

where  $c_2 > 0$  is the constant corresponding to  $L, \gamma_l$  and  $1 < q < 2$ . According to the local error bound condition, the following inequality holds:

$$\|F(\mathcal{P}_{\theta K, lK, \rho K, \sigma}(\mathbf{w}^K + \mathbf{d}^K))\| \leq \tilde{c}_2 \gamma_l \text{dist}(\mathbf{w}^K, \mathbf{W}_*)^q \leq \tilde{c}_2 \gamma_l^{1-q} \|F(\mathbf{w}^K)\|^q. \quad (45)$$

According to Theorem 4, we have  $\|F(\mathbf{w}^k)\| \rightarrow 0$ . Consequently, there exists  $\delta_{\hat{\mathbf{w}}_*, 5}$  such that for  $\mathbf{w}^K \in B(\hat{\mathbf{w}}_*, \delta_{\hat{\mathbf{w}}_*, 5})$ ,  $\|F(\mathbf{w}^K)\|^{q-1} < \frac{1}{\tilde{c}_2 \gamma_l^{1-q} \nu}$ . It follows that

$$\|F(\mathcal{P}_{\theta K, lK, \rho K, \sigma}(\mathbf{w}^K + \mathbf{d}^K))\| < \nu \|F(\mathbf{w}^K)\|$$

and hence (15) holds. Furthermore, it follows from the proof of (Hu et al., 2025, Theorem 6) that there exists  $\delta_{\hat{\mathbf{w}}_*,6}, \mathbf{w}^{K+1} \in B(\hat{\mathbf{w}}_*, \delta_{\hat{\mathbf{w}}_*,6})$  if  $\mathbf{w}^K \in B(\hat{\mathbf{w}}_*, \delta_{\hat{\mathbf{w}}_*,6})$ . Consequently, let  $\delta_{\hat{\mathbf{w}}_*} = \min\{\delta_{\hat{\mathbf{w}}_*,1}, \delta_{\hat{\mathbf{w}}_*,2}, \delta_{\hat{\mathbf{w}}_*,3}, \delta_{\hat{\mathbf{w}}_*,4}, \delta_{\hat{\mathbf{w}}_*,5}, \delta_{\hat{\mathbf{w}}_*,6}\}$  and it follows that (C1) holds by induction.

(C2): By Lemma 7,  $F$  is smooth locally at  $\hat{\mathbf{w}}_* \in \mathbf{W}_*$  on  $\overline{\mathcal{M}}_{\hat{\mathbf{w}}_*}$ . According to the proof in (C1), condition (Hu et al., 2025, Assumption 3(A1)) holds for  $\mathbf{w}^k, \mathbf{w}^{k+1}, k > K$ . It then follows from (44) and (Hu et al., 2025, Theorem 6) that  $\{\mathbf{w}^k\}$  is a Cauchy sequence and hence converges to some  $\mathbf{w}_* \in \overline{\mathcal{M}}_{\hat{\mathbf{w}}_*}$  superlinearly, which completes the proof of (C2). ■

**Remark 11** In Theorem 10, (C1) states that no line search is needed for  $k > K$  and (C2) presents the superlinear convergence results. The condition  $\mathbf{w}^k \in \overline{\mathcal{M}}_{\hat{\mathbf{w}}_*}$  is used to guarantee the smoothness of  $F$  and is also assumed in (Hu et al., 2025, Lemma 6). Furthermore, we prove that  $\mathbf{w}^k \in \overline{\mathcal{M}}_{\hat{\mathbf{w}}_*}$  for every  $k > K$ . If assumptions in Theorem 10 and the additional SC hold, then  $\theta, l, \rho$  are all equal to 0, which indicates the correction map  $\mathcal{P}_{\theta,l,\rho,\sigma}$  reduces to the identity operator and  $F$  is smooth locally on the whole space. Consequently, Theorem 10 is a theoretical extension compared with the local convergence results in (Hu et al., 2025; Deng et al., 2025), which rely on SC condition.

To gain a more concrete understanding of how restrictive SC is, we next present the SC of problem (1).

**Proposition 12** Denote  $\mathbf{w}_*$  as a solution. Under Assumption 1 and by (Mordukhovich and Nam, 2017, Theorem 6.2), SC holds at  $\mathbf{w}_*$  if and only if

$$\mathbf{z}_* \in \text{ri}(-\partial h(\mathbf{x}_*)), \mathbf{y}_* \in \text{ri}(-\mathcal{N}_{\mathcal{Q}}(\mathcal{A}(\mathbf{x}_*))), \mathbf{c} - \mathbf{z}_* - \mathbf{A}^* \mathbf{y}_* \in \text{ri}(-\mathcal{N}_{\mathcal{K}}(\mathbf{x}_*)), \quad (46)$$

where  $\mathcal{N}_{\mathcal{C}}(\mathbf{x}) := \{\mathbf{s} \mid \langle \mathbf{s}, \mathbf{p} \rangle \leq \langle \mathbf{s}, \mathbf{x} \rangle, \forall \mathbf{p} \in \mathcal{C}\}$  is the normal cone of the convex set  $\mathcal{C}$ . Furthermore, for SDP, SC reduces to

$$\text{rank}(\mathbf{x}_*) + \text{rank}(\mathbf{s}_*) = n, \langle \mathbf{x}_*, \mathbf{s}_* \rangle = 0. \quad (47)$$

For SDP+, SC simplifies to

$$\text{rank}(\mathbf{x}_*) + \text{rank}(\mathbf{s}_*) = n, \langle \mathbf{x}_*, \mathbf{s}_* \rangle = 0, \langle \mathbf{z}_*, \mathbf{x}_* \rangle = 0, \mathbf{x}_* + \mathbf{z}_* > 0. \quad (48)$$

**Proof** According to the definition of normal cone, we have  $\mathcal{N}_{\mathcal{K}}(\mathbf{x}_*) = \{\mathbf{s} \mid \langle \mathbf{s}, \mathbf{p} \rangle \leq \langle \mathbf{s}, \mathbf{x}_* \rangle, \forall \mathbf{p} \in \mathcal{K}\}$ . Through taking  $\mathbf{p} = \frac{1}{2}\mathbf{x}_*$  and  $2\mathbf{x}_*$ , it can be verified that  $\langle \mathbf{s}, \mathbf{x}_* \rangle = 0$  for all  $\mathbf{s} \in \mathcal{N}_{\mathcal{K}}(\mathbf{x}_*)$ . As a consequence,  $\mathcal{N}_{\mathcal{K}}(\mathbf{x}_*) = \{\mathbf{s} \mid \langle \mathbf{s}, \mathbf{p} \rangle \leq 0, \langle \mathbf{x}_*, \mathbf{s} \rangle = 0, \forall \mathbf{p} \in \mathcal{K}\} = -\mathcal{K}^* \cap \{\mathbf{x}_*\}^\perp$ , where  $\mathcal{K}^*$  denotes the dual cone of  $\mathcal{K}$ . Let  $\mathbf{x}_* = \sum_{i=1}^r \lambda_i V_i V_i^*$  be the eigenvalue decomposition, where  $r$  is the rank of  $\mathbf{x}_*$ ,  $\lambda_1, \dots, \lambda_r$  correspond to the eigenvalues and  $[V_1, \dots, V_r]$  are the corresponding eigenvectors. Denote  $[V_{r+1}, \dots, V_n]$  as the orthogonal basis of the orthogonal complement subspace of the space generated by  $[V_1, \dots, V_r]$ . We claim that

$$-\mathcal{K}^* \cap \{\mathbf{x}_*\}^\perp = \mathcal{S} := \{\mathbf{s} \mid \mathbf{s} = \sum_{i=1}^{n-r} \alpha_i V_{i+r} V_{i+r}^*, \alpha \leq 0\}. \quad (49)$$

We first prove that  $\mathcal{S} \subseteq -\mathcal{K}^* \cap \{\mathbf{x}_*\}^\perp$ . It is obvious that  $\langle \mathbf{s}, \mathbf{x} \rangle = 0$  since  $V_i^* V_j = 0$  for  $i \neq j$ . According to the definition of  $\mathcal{S}$ , for every  $-\mathbf{s} \in \mathcal{S}$ , we have  $\mathbf{s} \in \mathcal{K}^*$ . Then it follows that

$\mathcal{S} \subseteq \mathcal{N}_{\mathcal{K}}(\mathbf{x}_*)$ . For every  $\mathbf{s} \in -\mathcal{K}^* \cap \{\mathbf{x}_*\}^\perp$ , since  $-\mathbf{s}$  is a positive semidefinite matrix and the equality  $\langle \mathbf{s}, \mathbf{x}_* \rangle = 0$  is equivalent to  $\mathbf{x}_* \mathbf{s} = \mathbf{s} \mathbf{x}_* = 0$ , we have  $\mathbf{x}_*$  and  $\mathbf{s}$  are simultaneously diagonalizable. Hence we have that the corresponding eigenvalue  $\Lambda, \Lambda_s$  of  $\mathbf{x}_*$  and  $\mathbf{s}$  satisfy  $\Lambda \Lambda_s = 0$ . Consequently, there exist  $\alpha_1, \dots, \alpha_{n-r}$  such that  $\mathbf{s} = \sum_{i=1}^{n-r} \alpha_i V_{i+r} V_{i+r}^* \in \mathcal{S}$ , which means  $-\mathcal{K}^* \cap \{\mathbf{x}_*\}^\perp = \mathcal{S}$ . Since the affine hull of  $\mathcal{S}$  is  $\bar{\mathcal{S}} := \{\mathbf{s} | \mathbf{s} = \sum_{i=1}^{n-r} \alpha_i V_{i+r} V_{i+r}^*, \alpha > 0\}$ , it follows that  $-\text{ri}(\mathcal{N}_{\mathcal{K}}(\mathbf{x}_*)) = \{\mathbf{s} | \mathbf{s} = \sum_{i=1}^{n-r} \alpha_i V_{i+r} V_{i+r}^*, \alpha > 0\}$ , under which we can give examples where SC holds for concrete examples.

For the classical SDP problems, SC boils down to the fact that there exists  $\mathbf{s}_* = \mathbf{c} - \mathcal{A}^* \mathbf{y}_*$ , such that  $\mathbf{s}_* \in \text{ri}(\mathcal{K}^* \cap \{\mathbf{x}_*\}^\perp)$  (Rockafellar and Wets, 2009, Proposition 2.44). Hence the SC holds for SDP if and only if (47) holds. For SDP+ problem, since  $\mathcal{Q} = \{\mathbf{b}\}$ , and  $h(\mathbf{x}) = \delta_{\mathbf{x} \geq 0}(\mathbf{x})$ , the SC boils down to the fact that there exists  $\mathbf{z}_* \in -\text{ri}(\mathcal{N}_{\{\mathbf{x} \geq 0\}}(\mathbf{x}_*))$ ,  $\mathbf{s}_* = \mathbf{c} - \mathcal{A}^*(\mathbf{y}_*) - \mathbf{z}_*$ ,  $\mathbf{s}_* \in \text{ri}(\mathcal{K}^* \cap \{\mathbf{x}_*\}^\perp)$ . Analogously, the SC holds for SDP+ problem if and only if (48) holds.  $\blacksquare$

### 4.3 Complexity analysis

We now present the iteration complexity of Algorithm 1 by assuming that parameters  $\{\varsigma_k\}$  and  $\{\|\boldsymbol{\eta}^k\|\}$  are set properly.

**Theorem 13** *Suppose that Assumption 1 holds. Let  $\{\mathbf{w}^k\}$  be the sequence generated by Algorithm 1 with parameters  $\varsigma_k$  and  $\boldsymbol{\eta}^k$  such that  $\varsigma_k \leq Ck^{-\frac{5}{3}}$ ,  $\|\boldsymbol{\eta}^k\|^2 \leq Ck^{-2}$  for all  $k$ , where  $C > 0$  is a constant. Then for a given accuracy  $\varepsilon > 0$ , it holds that for at most  $K = \tilde{\mathcal{O}}(\varepsilon^{-3/2})$  iterations, we have*

$$\|F(\mathbf{w}^K)\|^2 \leq \varepsilon. \quad (50)$$

Furthermore, let  $\varepsilon_0$  be the threshold such that (44) holds and  $q$  be the exponent of the superlinear convergence. If the Assumption in Theorem 10 holds, (50) is satisfied after at most  $K = \tilde{\mathcal{O}}(\varepsilon_0^{-3/2}) + \mathcal{O}(\log_q(\log(\frac{\varepsilon_0}{\varepsilon})))$  iterations.

**Proof** We first consider the case where (16) happens with finite times. It follows from (34) that (50) holds with at most  $\mathcal{O}(\varepsilon^{-3/2})$  iterations in this case. The worst complexity of Algorithm 1 occurs in the case where the update of  $\mathbf{w}^{k+1}$  associated with (15) and (16) both happen infinitely many times. Since  $\sum_{j=1}^{\infty} \frac{4\kappa_1^2 L^2}{j^{3\beta}} < +\infty$ , there exists a large enough  $K$  independent of  $\varepsilon$  and a constant  $\bar{\nu} \in (\nu, 1)$  such that  $C := \sqrt{\prod_{j=K}^{\infty} \left(1 + \frac{4\kappa_1^2 L^2}{j^{3\beta}}\right)} \leq \sqrt{\exp(\sum_{j=K}^{\infty} \frac{4\kappa_1^2 L^2}{j^{3\beta}})} < \frac{\bar{\nu}}{\nu}$ . Let  $k_1, \dots, k_n$  be the indices corresponding to the steps associated with (15) is satisfied. Since for any  $k > 0$ ,  $\sum_{j=k+1}^{\infty} Cj^{-\frac{5}{3}} \leq C \int_k^{\infty} x^{-\frac{5}{3}} dx = Ck^{-\frac{2}{3}}$  and  $\sum_{j=k+1}^{\infty} Cj^{-\frac{7}{3}} \leq C \int_k^{\infty} x^{-7/3} dx = Ck^{-4/3}$ . Hence we need at most  $k = \mathcal{O}(\varepsilon^{-3/2})$  iterations such that  $\sqrt{\sum_{j=k}^{\infty} \frac{4C}{l^{7/3}}} \leq (b_2 - b_1)\varepsilon / [\zeta^2(1 - \bar{\nu})C]$  and  $\sum_{j=k}^{\infty} \varsigma_j \leq \sum_{j=k+1}^{\infty} \frac{C}{j^{5/3}} \leq b_1\varepsilon / [2\zeta^2(1 - \bar{\nu})]$ , where  $b_1 \in (0, 1)$ ,  $b_2 \in (b_1, 1)$  are two constants.

Let  $n_0$  be large enough such that  $\bar{\pi}_{n_0} := \sum_{j=k_{n_0}}^{\infty} \frac{C}{j^{7/3}} \leq (b_2 - b_1)\varepsilon / [2(1 - \bar{\nu})\zeta^2]$ . Subsequently, let  $n$  be large enough that  $n \geq n_0 + \zeta$  and  $k_n \geq K \geq 4$ . According to the proof of

Lemma 3 and (30), for any  $k_n \leq j < k_{n+1}$ ,

$$\begin{aligned}
\|F(\mathbf{w}^{j+1})\| &\leq \sqrt{\left(1 + \frac{4\kappa_1^2 L^2}{j^{3\beta}}\right) \|F(\mathbf{w}^j)\|^2 + \frac{2}{\tau_{k,i} - 1} \|\boldsymbol{\eta}^k\|^2} \\
&\leq \sqrt{\Pi_{k=k_n}^j \left(1 + \frac{4\kappa_1^2 L^2}{k^{3\beta}}\right) \|F(\mathbf{w}^{k_n})\|^2} + \sqrt{\Pi_{k=k_n}^j \left(1 + \frac{4\kappa_1^2 L^2}{k^{3\beta}}\right) \sum_{l=k_n}^j \frac{4C}{l^{7/3}}} \\
&\leq C \|F(\mathbf{w}^{k_n})\| + C \sqrt{\sum_{l=k_n}^j \frac{4C}{l^{7/3}}}.
\end{aligned}$$

Since  $\nu C \leq \bar{\nu}$ , it follows from the definition of  $C$  and  $\bar{\pi}_j$  that

$$\begin{aligned}
\|F(\mathbf{w}^{k_{n+1}})\| &\leq \nu \max_{\max(1, n-\zeta+1) \leq j \leq n} \left( C \|F(\mathbf{w}^{k_j})\| + \bar{\pi}_j + \varsigma_{k_j} \right) \\
&\leq \bar{\nu} a_n + \nu \max_{\max(1, n-\zeta+1) \leq j \leq n} (\varsigma_{k_j} + \bar{\pi}_j).
\end{aligned} \tag{51}$$

Subsequently, by the definition of  $c_n$  in Theorem 4, we have

$$\begin{aligned}
c_{n+1} &\stackrel{(51)}{\leq} \bar{\nu} c_n + \nu \sum_{l=n\zeta}^{(n+1)\zeta-1} \max_{\max(1, l-\zeta+1) \leq j \leq l} (\bar{\pi}_j + \varsigma_{k_j}) \leq \bar{\nu} c_n + \bar{\nu} \zeta^2 \bar{\pi}_{n\zeta} + \bar{\nu} \zeta^2 \sum_{j=k_{\zeta(n-1)}}^{k_{\zeta(n+1)}} \varsigma_j \\
&\leq \bar{\nu}^{n-n_0} c_{n_0} + \zeta^2 \sum_{j=k_{n_0}}^{k_{\zeta(n+1)}} \bar{\nu}^{k-j+1} \bar{\pi}_j + 2\zeta^2 \sum_{j=k_{n_0}}^{k_{\zeta(n+1)}} \bar{\nu}^{k-j} \varsigma_{k_j} \\
&\leq \bar{\nu}^{n-n_0} c_{n_0} + (b_2 - b_1)\varepsilon + b_1\varepsilon = \bar{\nu}^{n-n_0} c_{n_0} + b_2\varepsilon,
\end{aligned}$$

where the last equality follows from the definition of  $\bar{\pi}_j$  and the assumption of  $\varsigma_j$ . This implies that we need at most  $\mathcal{O}(\log(\frac{1}{\varepsilon}))$  iterations of (16) to make  $\|F(\mathbf{w}^{k_n})\|^2 \leq \varepsilon$ . By (34), we have  $k_{n+1} - k_n \leq \mathcal{O}(\varepsilon^{-3/2})$ . Therefore, the overall complexity is  $\mathcal{O}(\varepsilon^{-3/2} \log(\frac{1}{\varepsilon})) + \mathcal{O}(\varepsilon^{-3/2})$ , dubbed as  $\tilde{\mathcal{O}}(\varepsilon^{-3/2})$ .

Furthermore, if the Assumption in Theorem 10 holds, it follows from (45) that there exists  $K_1 > 0$  such that  $\|F(\mathbf{w}^{k+1})\|^2 \leq \tilde{c}_2^2 \gamma_l^{2-2q} \|F(\mathbf{w}^k)\|^{2q}$ , where  $q \in (1, 2]$  for  $k > K_1$ . Hence (50) holds with at most  $\mathcal{O}(\log_q(\log(\frac{\varepsilon_0}{\varepsilon})))$  iterations. The proof is completed.  $\blacksquare$

## 5 Numerical experiments

To evaluate the effectiveness of SSNCP, we conduct extensive numerical experiments and compare it with state-of-the-art solvers SDPNAL+ (Sun et al., 2020) and MOSEK (ApS, 2019) comprehensively. We implement SSNCP using MATLAB R2023b. All experiments are performed on a Linux server with a sixteen-core Intel Xeon Gold 6326 CPU and 256 GB memory.

### 5.1 Experiments setting

Consistent with the metrics commonly used to test for SDP problems (Yang et al., 2015), we evaluate the performance of SSNCP for SDP via the following quantity:

$$\eta_1 = \max\{\eta_p, \eta_d, \eta_{\mathcal{K}}, \eta_{\mathcal{K}^*}, \eta_{C_1}\},$$

where  $\mathbf{s} = \Pi_{\mathcal{K}}(\mathbf{c} - \mathcal{A}^*(\mathbf{y}) - \mathbf{z} - \mathbf{x})$ ,

$$\begin{aligned} \eta_p &= \frac{\|\mathcal{A}(\mathbf{x}) - \mathbf{b}\|}{1 + \|\mathbf{b}\|}, \eta_d = \frac{\|\mathcal{A}^*(\mathbf{y}) + \mathbf{z} + \mathbf{s} - \mathbf{c}\|}{1 + \|\mathbf{c}\|}, \\ \eta_{\mathcal{K}} &= \frac{\|\mathbf{x} - \Pi_{\mathcal{K}}(\mathbf{x})\|}{1 + \|\mathbf{x}\|}, \eta_{\mathcal{K}^*} = \frac{\|\mathbf{s} - \Pi_{\mathcal{K}^*}(\mathbf{s})\|}{1 + \|\mathbf{s}\|}, \eta_{C_1} = \frac{|\langle \mathbf{x}, \mathbf{s} \rangle|}{1 + \|\mathbf{x}\| + \|\mathbf{s}\|}. \end{aligned} \quad (52)$$

For SDP+ problems, we evaluate the performance of the tested algorithms via the following quantity

$$\eta_2 = \max\{\eta_p, \eta_d, \eta_{\mathcal{K}}, \eta_{\mathcal{K}^*}, \eta_{C_1}, \eta_{\mathcal{P}}, \eta_{C_2}\},$$

where  $\eta_p, \eta_d, \eta_{\mathcal{K}}, \eta_{\mathcal{K}^*}, \eta_{C_1}$  are defined in (52),  $\eta_{\mathcal{P}} = \frac{\|\Pi_{\mathcal{P}^*}(-\mathbf{x})\|}{1 + \|\mathbf{x}\|}$ , and  $\eta_{C_2} = \frac{|\langle \mathbf{x}, \mathbf{z} \rangle|}{1 + \|\mathbf{x}\| + \|\mathbf{z}\|}$ . We stop SSNCP for SDP when  $\eta_1 < 10^{-6}$  and SDP+ when  $\eta_2 < 10^{-6}$ . We note that  $\mathbf{z} \equiv \mathbf{0}$  in (52) for SDP problems. Furthermore, we also compute the relative gap  $\eta_g := \frac{|\text{obj}_P - \text{obj}_D|}{1 + \text{obj}_P + \text{obj}_D}$ , where  $\text{obj}_P$  and  $\text{obj}_D$  denote the primal and dual objective function value.

### 5.2 Numerical validation of theoretical results

In this subsection, we verify the effectiveness of the correction step in Algorithm 1 for problems without SC. For SDP case, we generate the solution  $\mathbf{x}_*$  and  $\mathbf{s}_*$  to be the diagonal matrices with  $\text{rank}(\mathbf{x}_*) + \text{rank}(\mathbf{s}_*) < n$ . We next set  $\mathbf{b} = \mathcal{A}\mathbf{x}_*$ ,  $\mathbf{c} = \mathcal{A}^*\mathbf{y}_* + \mathbf{s}_*$  where  $\mathcal{A}$  and  $\mathbf{y}_*$  are random sparse matrix and vector, respectively. For the SDP+ case, the solution  $\mathbf{x}_*$  and  $\mathbf{s}_*$  are generated in the same way as in the SDP problem and  $\mathbf{z}_*$  is a random nonnegative matrix with diagonal elements being 0. We also set  $\mathbf{b} = \mathcal{A}\mathbf{x}_*$ ,  $\mathbf{c} = \mathcal{A}^*\mathbf{y}_* + \mathbf{s}_* + \mathbf{z}_*$ . According to (47), (48) and the setting of the problems, SC does not hold for these tested problems.

In the following examples for SDP and SDP+ problems, we specify the parameter choices used in the algorithm. For SDP problems, the projection depends only on  $\theta^k$ , with  $\bar{\theta} = 1$  determined by the choices of diagonal matrices  $\mathbf{x}_*$  and  $\mathbf{s}_*$ . We set  $\theta^k = 0.05$  when  $\|F(\mathbf{w}^k)\| < 10^{-3}$ , and  $\theta^k = 0$  otherwise, so that the projection reduces to the identity in early iterations. For SDP+ problems, the projection depends on both  $\theta^k$  and  $\rho^k$ , with  $\bar{\theta} = \bar{\rho} = 1$  determined by  $\mathbf{x}_*$ ,  $\mathbf{s}_*$  and  $\mathbf{z}_*$ . We set  $\theta^k = \rho^k = 0.05$  when  $\|F(\mathbf{w}^k)\| < 10^{-3}$ , and 0 otherwise. In both cases, we set  $\|\boldsymbol{\eta}^k\| = 10^{-12}$  for all  $k$ , ensuring that Assumptions (A2) and (A3) are satisfied. Algorithm 1 terminates when either  $\eta_1 < 10^{-12}$  or  $\eta_2 < 10^{-12}$ .

The numerical results are presented in Figure 1. We conjecture from the last column that the local error bound condition (A1) holds, namely,  $\text{dist}(\mathbf{w}, \mathbf{w}_*) \leq \|\mathbf{w} - \mathbf{w}_*\| < \|F(\mathbf{w}^k)\|$  when  $\mathbf{w}^k$  is close to  $\mathbf{w}_*$ . This suggests that all conditions stated in Assumption 1 are satisfied. It is shown that the iterate sequence without a correction step exhibits oscillations, while the iteration points with a correction step avoid this problem. Furthermore, the superlinear convergence rate is observed, which verifies the conclusion of Theorem 10.

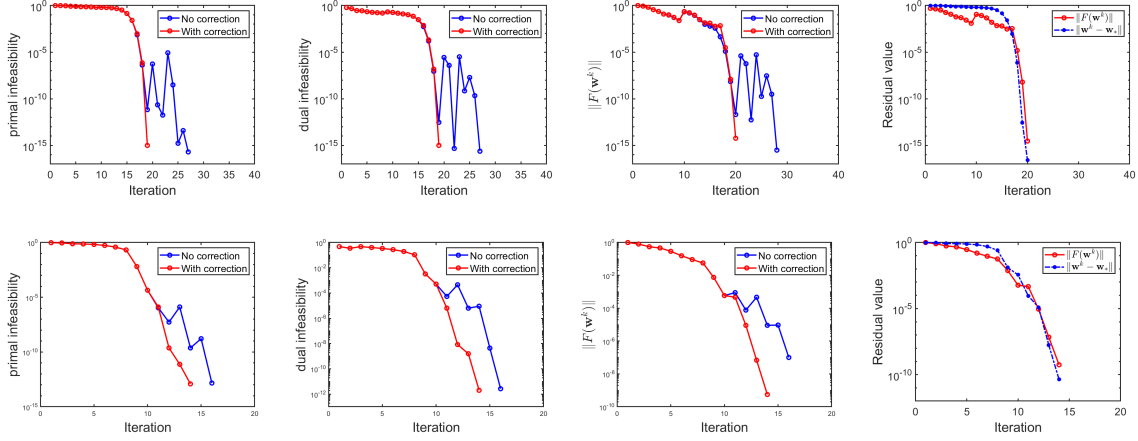


Figure 1: The first three columns: the performance of SSNCP for SDP (top row) and SDP+ (bottom row) problems with or without the correction step. The last column:  $\|F(\mathbf{w}^k)\|$  and  $\|\mathbf{w}^k - \mathbf{w}_*\|$  of SSNCP with correction step.

### 5.3 Lovász Theta problem

Let  $G = (V, E)$  be a simple, undirected graph. The Lovász theta problem (Sloane, 2005; Trick et al., 1992) is defined as

$$\theta(G) = \min_X \langle -ee^T, X \rangle, \text{ s.t. } \text{tr}(X) = 1, X \succeq 0, X_{ij} = 0, (i, j) \in E,$$

which is a SDP problem. The dimension  $n$  of the tested problems varies from 64 to 4096 and the number of constraints  $m$  varies from 513 to 504452. The numerical results are listed in Figure 2 and Table 1. As shown in Figure 2, compared with MOSEK and SDPNAL+, SSNCP successfully solve all 69 problems while MOSEK can only solve 73.9% of them due to the limited memory. The “error” means the comparison of residual error  $\eta_1$ . According to Table 1, SSNCP is faster than SDPNAL+ and MOSEK on 71.0 % of the 69 tested problems. Particularly, for large-scale problems such as 1zc.4096 and 2dc.2048, where  $(m, n) = (92161, 4096)$  and  $(504452, 2048)$ , respectively, SSNCP is two times faster than SDPNAL+ while MOSEK can not solve them due to the lack of memory.

Table 1: A statistic of computational results of tested algorithms for Theta problems

	SSNCP		SDPNAL+		MOSEK	
success	69	100.0%	68	98.6%	51	73.9%
fastest	49	71.0%	1	1.4%	19	27.5%
fastest under success	49	71.0%	1	1.5%	17	33.3%
not slower 3 times	69	100.0%	36	52.2%	25	36.2%
not slower 3 times under success	69	100.0%	46	67.6%	23	45.1%



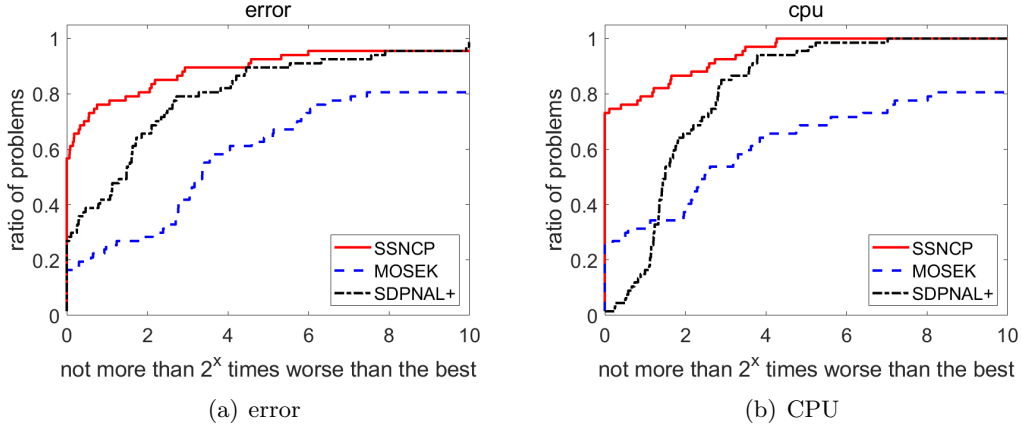


Figure 2: The performance profiles of tested algorithms for Theta problems

#### 5.4 Lovász Theta+ problem

Given a graph  $G$  with the edge set  $\mathcal{E}$ , the SDP+ relaxation of the maximum stable set problem (Sloane, 2005; Trick et al., 1992) is given by:

$$\theta_+(G) = \min\{\langle -ee^T, X \rangle : \text{tr}(X) = 1, X \succeq 0, X_{ij} = 0, (i, j) \in E, X \in \mathcal{P}\},$$

where the polyhedral cone  $\mathcal{P} = \{X \in \mathbb{S}^n | X \geq 0\}$ . The numerical results are listed in Figure 3 and Table 2, where “error” means the comparison of residual error  $\eta_2$ . It is shown in Figure 3 that SSNCP and SDPNAL+ can solve all the problems successfully while MOSEK cannot due to the lack of memory. In summary, SSNCP achieves higher accuracy than SDPNAL+ and MOSEK on most problems. According to the recorded outputs of all algorithms, SSNCP is faster than SDPNAL+ and MOSEK on 72.5% of the 69 problems.

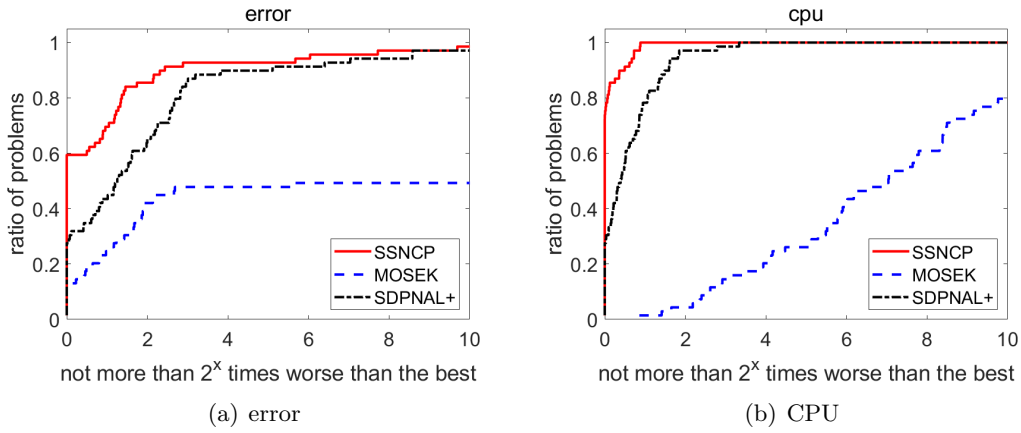


Figure 3: The performance profiles of tested algorithms for Theta+ problems

Table 2: A statistic of computational results of tested algorithms for Theta+ problems

	SSNCP		SDPNAL+		MOSEK	
success	69	100.0%	69	100.0%	13	18.8%
fastest	50	72.5%	19	27.5%	0	0.0%
fastest under success	50	72.5%	19	27.5%	0	0.0%
not slower 3 times	69	100.0%	62	89.9%	2	2.9%
not slower 3 times under success	69	100.0%	62	89.9%	1	7.7%

### 5.5 Rank-1 tensor approximations (R1TA)

The dual form of the R1TA problem (Nie and Wang, 2014) is given by

$$\min_{x \in \mathbb{R}} x, \quad \text{s.t. } xg - f = M^*(X), X \in \mathbb{S}_+^n, \quad (53)$$

which is a standard SDP (Nie and Wang, 2012), where the linear map  $\mathcal{A}$  depends on  $M, f$  and  $g$ . Figure 4 presents the performance profiles of the tested algorithms, which shows that SSNCP is the fastest in nearly all problems and MOSEK can not. Particularly, for large-scale problems such as nonsym(20,4) and nonsym(21,4), where the corresponding  $(m, n) = (12326390, 9261)$  and  $(9260999, 8000)$ , respectively, SSNCP is able to solve these problems successfully in less than 2 hours while both SDPNAL+ and MOSEK fail. As shown in Table 3, SSNCP can solve all the tested problems while MOSEK can not due to limited memory.

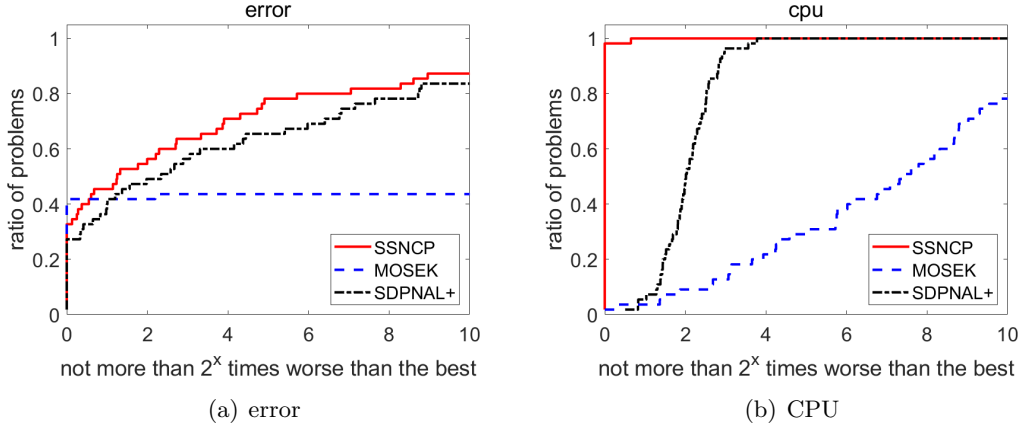


Figure 4: The performance profiles of tested algorithms for R1TA problems

### 5.6 Reduced density matrix (RDM) formulation problem

The RDM formulation for the electronic structure calculation problem is formulated as the constrained minimization of the total energy of the molecular system subject to the

Table 3: A statistic of computational results of tested algorithms for R1TA problems

	SSNCP		SDPNAL+		MOSEK	
success	55	100.0%	52	94.5%	25	45.5%
fastest	54	98.2%	0	0.0%	1	1.8%
fastest under success	54	98.2%	0	0.0%	1	4.0%
not slower 3 times	55	100.0%	14	25.5%	3	5.5%
not slower 3 times under success	55	100.0%	12	23.1%	2	8.0%

N-representability condition as an SDP (Li et al., 2018):

$$\begin{aligned}
& \min_{y, S_j} \quad b^T y, \\
& \text{s.t.} \quad S_j = \mathcal{A}_j^* y - C_j, j = 1, \dots, l, B^T y = c, \\
& \quad \quad 0 \preceq S_1 \preceq I, \quad 0 \preceq S_j, \quad j = 2, \dots, l.
\end{aligned} \tag{54}$$

We compared SSNCP, SDPNAL+, MOSEK, and SSNSDP (Li et al., 2018) on the RDM dataset. The test results are shown in Figure 5. According to Table 4, SSNCP returns solutions with accuracy under  $10^{-6}$  in all cases. Furthermore, SSNCP is faster than SDPNAL+, MOSEK, and SSNSDP on 55.8% of the 276 problems.

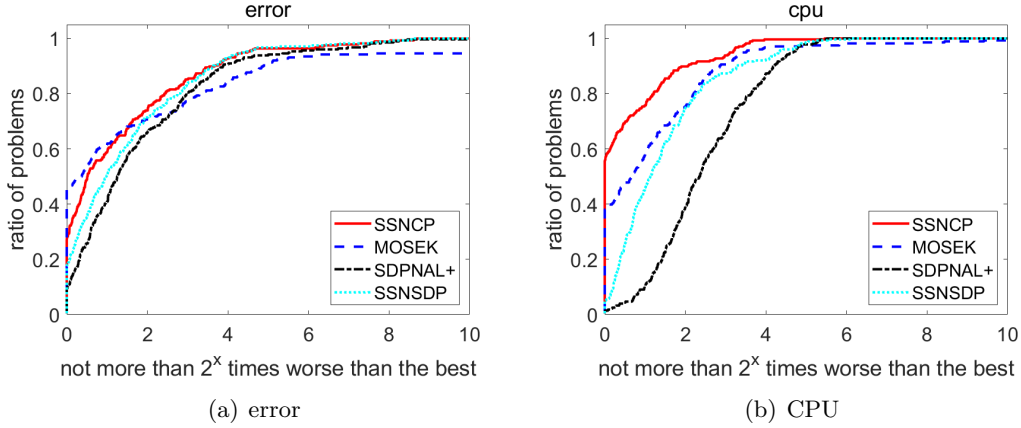


Figure 5: The performance profiles of tested algorithms for RDM problems

Table 4: A statistic of computational results of tested algorithms for RDM problems

	SSNCP		SDPNAL+		SSNSDP		MOSEK	
success	276	100.0%	239	86.6%	276	100.0%	243	88.0%
fastest	154	55.8%	3	1.1%	14	5.1%	105	38.0%
fastest under success	154	55.8%	5	2.1%	18	6.5%	103	42.4%
not slower 3 times	273	98.9%	103	37.3%	225	81.5%	190	68.8%
not slower 3 times under success	271	98.2%	98	41.0%	225	81.5%	180	74.1%

### 5.7 Binary integer nonconvex quadratic programming

Consider the SDP+ problem coming from the relaxation of a binary integer nonconvex quadratic (BIQ) programming. The relaxed problem has the following form (Burer, 2009):

$$\begin{aligned} \min_X \quad & \frac{1}{2} \langle Q, X_0 \rangle + \langle c, x \rangle, \\ \text{s.t.} \quad & \text{diag}(X_0) - x = 0, \alpha = 1, X = \begin{bmatrix} X_0 & x \\ x^T & \alpha \end{bmatrix} \in \mathbb{S}_+^n, \quad X \in \mathcal{P}, \end{aligned} \quad (55)$$

where the polyhedral cone  $\mathcal{P} = \{X \in \mathbb{S}^n \mid X \geq 0\}$ . In our numerical experiments, the 135 test data for  $Q$  and  $c$  are taken from the Biq Mac Library<sup>1</sup>. The numerical results are listed in Figure 6 which shows that SSNCP and SDPNAL+ can both solve all the problems. According to the recorded outputs of all algorithms, SSNCP is faster than SDPNAL+ and MOSEK on 80.0% of the 135 problems.

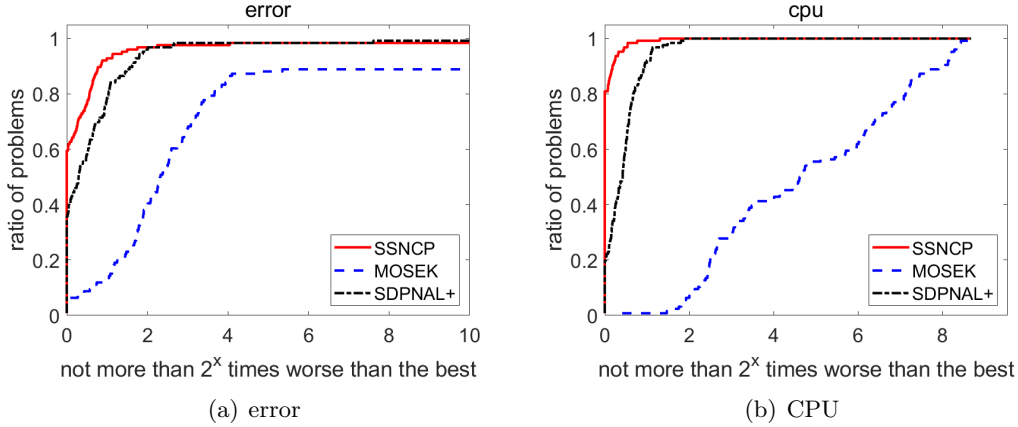


Figure 6: The performance profiles of tested algorithms for BIQ problems

Table 5: A statistic of computational results of tested algorithms for BIQ problems

	SSNCP		SDPNAL+		MOSEK	
success	135	100.0%	133	98.5%	73	54.1%
fastest	108	80.0%	27	20.0%	0	0.0%
fastest under success	108	80.0%	27	20.3%	0	0.0%
not slower 3 times	133	98.5%	133	98.5%	3	2.2%
not slower 3 times under success	133	98.5%	131	98.5%	1	1.4%

### 5.8 Relaxation of clustering problems

The SDP+ relaxation of clustering problems (RCP) described in (Peng and Wei, 2007) can be represented as

1. <http://biqmac.uni-klu.ac.at/biqmaclib.html>.

$$\min \langle -W, X \rangle, \text{ s.t. } Xe = e, \text{tr}(X) = K, X \geq 0, X \succeq 0. \quad (56)$$

where  $W$  is the affinity matrix whose entries represent the similarities of the objects in the dataset,  $e$  is the vector of ones, and  $K$  is the number of clusters. All the datasets we tested are selected from the UCI Machine Learning Repository<sup>2</sup>, including “abalone”, “segment”, “soybean” and “spambase”. The numerical results comparing with SDPNAL+ and MOSEK are shown in Figure 7 and Table 5, these figures again show that the accuracy and the CPU time of SSNCP are better than SDPNAL+ on most problems. According to Table 5, SSNCP is faster than SDPNAL+ and MOSEK on 76.7% of the 120 problems.

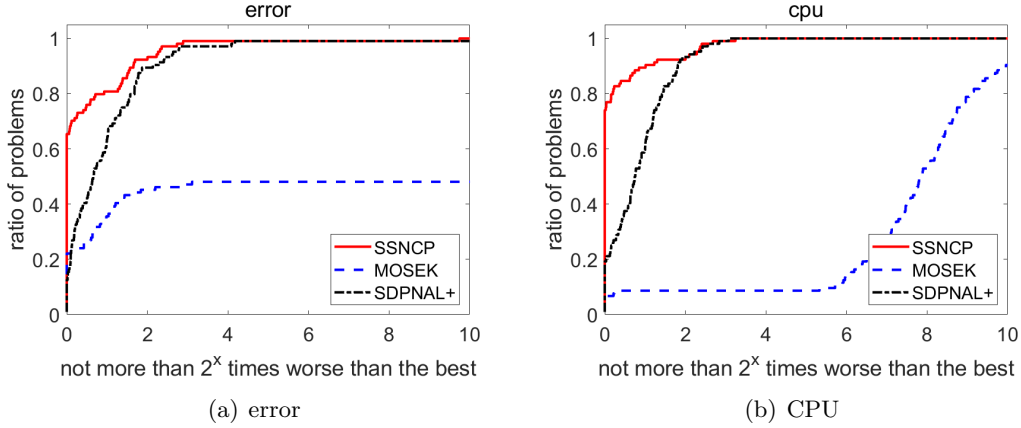


Figure 7: The performance profiles of tested algorithms for RCP problems

Table 6: A statistic of computational results of tested algorithms for RCP problems

	SSNCP		SDPNAL+		MOSEK	
success	120	100.0%	120	100.0%	36	30.0%
fastest	92	76.7%	20	16.7%	8	6.7%
fastest under success	92	76.7%	20	16.7%	3	8.3%
not slower 3 times	115	95.8%	100	83.3%	10	8.3%
not slower 3 times under success	115	95.8%	103	85.8%	5	13.9%

### 5.9 Mittelman benchmark

The Mittelman benchmark<sup>3</sup> is widely recognized as the most authoritative benchmark for SDP, where numerous commercial solvers are tested. In our experiments, all solvers run on four CPUs with 16GB in total. We stop SSNCP, SDPNAL+ and MOSEK when  $\eta_1 < 10^{-6}$ . For problems that are difficult to achieve high precision or when stagnation occurs, we stop the SSNCP at a medium accuracy. For consistency, different from the setting of SDP stated in Section 5.1, we use the same criteria as Mittelman’s benchmark. To be

2. <http://archive.ics.uci.edu/ml/datasets.html>

3. [https://plato.asu.edu/ftp/sparse\\_sdp.html](https://plato.asu.edu/ftp/sparse_sdp.html)

specific, the “success-1e-2” means the number of solutions that satisfy  $\min\{\eta_1, \eta_g\} < 10^{-2}$  while “success-1e-4” denotes the number of solutions that satisfy  $\eta_1 < 10^{-4}$ . We note that the criterion “success-1e-2” is also used in the test of the Mittelmann benchmark<sup>3</sup> to decide whether a problem is solved. The maximum iteration time is set as  $2 \times 10^4$  seconds and the maximum number of iterations is  $10^5$ . In order to better demonstrate the efficiency of our algorithm, different parameters are chosen for challenging classes of problems for SSNCP.

The results of the numerical experiments are listed in Figure 8 and Table 8. The geomean over all instances is calculated by  $\text{geomean} = (\prod_{i=1}^n (t_i + \zeta_0))^{\frac{1}{n}} - \zeta_0$ , where  $n$  denotes the number of instances,  $t_i$  denotes the time consumed by the  $i$ -th instance and  $\zeta_0 > 0$  is a small value to avoid the case that  $t_i$  is small. We set  $\zeta_0 = 10$  seconds in the computation which is the same as the Mittelmann benchmark. These figures show that SSNCP is competitive with MOSEK and SDPNAL+ on the challenging Mittelmann benchmark on CPU time and accuracy. Furthermore, it is shown in Table 8 that on all the 75 tested problems, the geometric mean time of SSNCP is significantly lower than that of SDPNAL+, especially MOSEK. The results demonstrate that SSNCP has the potential to solve challenging large-scale SDP. Specifically, for challenging problems arising from Theta dataset such as the **1et.2048** and **1tc.2048** problems, SSNCP can solve them in less than 40 minutes, which is twice faster than SDPNAL+ while MOSEK cannot due to limited memory. For problems arising from minimum bisection or max-cut problems such as **G60mb** and **G60mc**, SSNCP is able to solve them in less than 1 hour while MOSEK needs more than 3 hours to solve them. In addition, for problems with large  $m$  such as **hamming956** and **theta123**, MOSEK fails to solve them due to the lack of memory while SSNCP can solve them in less than 5 seconds.

Table 7: Selected computational results of tested algorithms on Mittelmann benchmark.

id	m	n	SSNCP				SDPNAL+				MOSEK			
			$\eta_p$	$\eta_d$	iter	time	$\eta_p$	$\eta_d$	iter	time	$\eta_p$	$\eta_d$	iter	time
G40mb	2000	2001	3.6e-07	2.0e-08	117	<b>94.2</b>	7.6e-07	8.4e-07	12319	9954.6	2.7e-06	1.7e-07	24	288.9
G48mb	3000	3001	1.3e-10	2.5e-08	125	<b>227.2</b>	1.6e-07	6.8e-07	1511	2207.0	2.7e-13	1.8e-14	8	304.2
G48mc	3000	3000	5.8e-08	9.2e-07	96	<b>170.1</b>	4.4e-07	9.3e-07	1942	2667.5	2.5e-14	2.4e-09	7	175.8
G55mc	5000	5000	1.2e-08	1.0e-07	86	<b>1158.9</b>	8.2e-07	8.2e-07	1098	9769.8	5.6e-13	1.4e-07	13	1474.9
G59mc	5000	5000	3.5e-07	1.3e-07	84	<b>1153.8</b>	1.7e-14	6.5e-07	1018	10003.4	6.4e-13	6.9e-07	12	1402.3
G60mb	7000	7001	4.5e-07	1.0e-07	46	<b>3563.8</b>	3.4e-03	2.1e-03	136	10020.4	5.8e-06	4.8e-08	25	14019.8
G60mc	7000	7001	4.5e-07	1.0e-07	45	<b>3561.7</b>	5.8e-03	9.6e-03	134	10082.5	5.8e-06	4.8e-08	25	13559.0
1dc.1024	1024	24064	7.2e-07	5.5e-07	38	<b>57.1</b>	9.2e-07	7.5e-07	113	160.7	8.4e-09	2.5e-09	12	421.5
1et.2048	2048	22529	8.4e-07	3.7e-07	77	<b>1069.1</b>	8.3e-07	3.7e-07	841	2211.4	NaN	NaN	NaN	NaN
1tc.2048	2048	18945	5.1e-07	7.9e-07	123	<b>2250.9</b>	9.9e-07	2.3e-07	1331	4471.6	NaN	NaN	NaN	NaN
1zc.1024	1024	16641	6.4e-07	1.4e-07	19	<b>5.8</b>	2.8e-07	5.8e-07	107	38.6	5.2e-10	5.0e-10	9	148.2
AlH1-	5990	7230	6.1e-07	5.0e-07	58	<b>116.5</b>	7.9e-07	1.0e-06	1610	1907.8	7.3e-09	5.1e-09	24	1402.2
BH22	2166	1743	3.3e-07	9.9e-07	96	<b>30.5</b>	3.4e-07	9.8e-07	3423	230.0	5.5e-09	3.4e-09	28	42.8
Bex215	2112	3002	2.5e-08	3.2e-08	29	<b>11.0</b>	7.9e-07	6.9e-07	228	64.7	3.1e-09	1.1e-10	11	11.7
Bstjcbpaf2	2244	3002	1.5e-06	1.8e-07	26	<b>14.1</b>	6.2e-09	2.6e-07	215	41.3	4.1e-08	1.5e-09	15	18.6
CH21A1	2166	1743	1.3e-07	7.5e-07	98	<b>34.7</b>	5.3e-07	9.9e-07	2417	188.9	8.0e-09	5.0e-09	25	44.8
H3O+1-	3162	2964	4.3e-07	8.8e-07	63	<b>105.3</b>	9.1e-07	1.0e-06	3206	551.1	6.7e-09	4.1e-09	23	395.7
NH2-	2044	1743	4.4e-07	8.7e-07	44	<b>19.8</b>	8.3e-07	8.4e-07	1104	101.5	4.9e-10	2.0e-06	38	55.7
NH31-	3162	2964	5.3e-08	9.8e-07	73	<b>66.2</b>	3.4e-07	1.0e-06	2900	436.1	5.3e-09	3.1e-09	23	212.4
NH4+	4236	4743	4.9e-08	6.7e-07	90	<b>286.1</b>	3.3e-09	1.0e-06	2767	831.9	5.3e-09	1.8e-06	46	818.8
biomedP	6514	6515	8.8e-07	8.6e-07	131	<b>5753.2</b>	1.2e-04	7.0e-04	286	10009.6	5.2e-04	6.7e-08	23	12682.2
fap09	174	30276	1.0e-04	9.4e-07	94	<b>5.8</b>	2.8e-07	9.0e-07	1010	8.3	2.6e-09	1.7e-03	23	1489.0
hamming834	256	16129	1.2e-07	7.3e-18	8	<b>0.1</b>	5.9e-08	5.8e-07	23	1.2	1.4e-11	2.3e-13	5	55.2
hamming956	513	53761	1.9e-08	3.5e-08	10	<b>0.5</b>	6.9e-07	9.2e-07	102	5.3	0.0e+00	NaN	NaN	NaN

Table 8: A statistic of computational results of tested algorithms for Mittelmann benchmark.

	SSNCP		SDPNAL+		MOSEK	
success-1e-2	68	90.7%	50	66.7%	67	88.3%
success-1e-4	64	85.3%	48	64.0%	62	82.7%
fastest	45	60.0%	2	2.7%	28	37.3%
shifted geomean time	<b>226.9</b>		800.2		336.9	

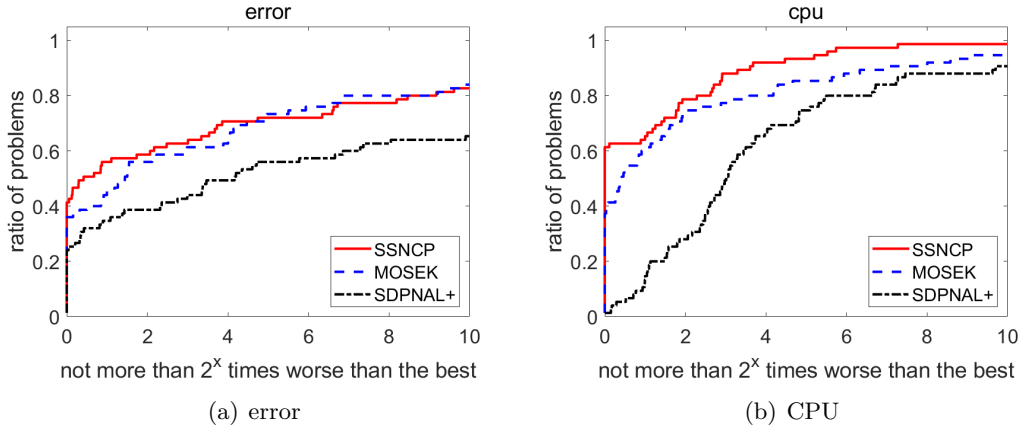


Figure 8: The performance profiles of tested algorithms on Mittelmann benchmark

## 6 Conclusion

In this paper, we introduce a novel semismooth Newton method, SSNCP, to solve SDP. Our method derives from a semismooth system based on the saddle point problem utilizing the augmented Lagrangian duality. To overcome difficulties associated with nonsmoothness, we incorporate a correction step to ensure that the iterates reside on a manifold where the nonlinear mapping exhibits smoothness. Global convergence is achieved by incorporating carefully designed inexact criteria and by exploiting the  $\alpha$ -averaged property of the semismooth mapping. Moreover, SSNCP achieves a superlinear convergence rate under the local error bound condition without relying on the stringent nonsingularity or strict complementarity conditions. Additionally, we demonstrate that SSNCP converges to an  $\varepsilon$ -stationary point with an iteration complexity of  $\tilde{O}(\varepsilon^{-3/2})$ . Numerical experiments on a variety of datasets, including the Mittelmann benchmark, highlight the efficiency and effectiveness of SSNCP compared to state-of-the-art solvers.

## References

M. F. Anjos and J. B. Lasserre. *Handbook on semidefinite, conic and polynomial optimization*, volume 166. Springer Science & Business Media, 2011.

- M. ApS. *The MOSEK optimization toolbox for MATLAB manual. Version 10.1.0.*, 2019.  
URL <http://docs.mosek.com/10.1/toolbox/index.html>.
- P. Armand and R. Omh  ni. A globally and quadratically convergent primal–dual augmented Lagrangian algorithm for equality constrained optimization. *Optimization Methods and Software*, 32(1):1–21, 2017.
- G. Bareilles, F. Iutzeler, and J. Malick. Newton acceleration on manifolds identified by proximal gradient methods. *Mathematical Programming*, 200(1):37–70, 2023.
- A. Beck. *First-order Methods in Optimization*. SIAM, 2017.
- N. Boumal. *An Introduction to Optimization on Smooth Manifolds*. Cambridge University Press, 2023.
- S. Burer. On the copositive representation of binary and continuous nonconvex quadratic programs. *Mathematical Programming*, 120(2):479–495, 2009.
- S. Burer and R. D. Monteiro. A nonlinear programming algorithm for solving semidefinite programs via low-rank factorization. *Mathematical Programming*, 95(2):329–357, 2003.
- D. de Roux, R. Carr, and R. Ravi. Instance-specific linear relaxations of semidefinite optimization problems. *Mathematical Programming Computation*, pages 1–51, 2025.
- Z. Deng, K. Deng, J. Hu, and Z. Wen. An augmented Lagrangian primal-dual semismooth Newton method for multi-block composite optimization. *Journal of Scientific Computing*, 102(3):65, 2025.
- L. Ding and M. Udell. A strict complementarity approach to error bound and sensitivity of solution of conic programs. *Optimization Letters*, 17(7):1551–1574, 2023.
- D. Drusvyatskiy and A. S. Lewis. Optimality, identifiability, and sensitivity. *Mathematical Programming*, 147(1-2):467–498, 2014.
- F. Feng, C. Ding, and X. Li. A quadratically convergent semismooth Newton method for nonlinear semidefinite programming without generalized jacobian regularity. *Mathematical Programming*, pages 1–41, 2025.
- J.-B. Hiriart-Urruty, J.-J. Strodiot, and V. H. Nguyen. Generalized Hessian matrix and second-order optimality conditions for problems with  $C^{1,1}$  data. *Applied mathematics and optimization*, 11(1):43–56, 1984.
- J. Hu, T. Tian, S. Pan, and Z. Wen. On the analysis of semismooth Newton-type methods for composite optimization. *Journal of Scientific Computing*, 103(2):1–31, 2025.
- W. Karush. Minima of functions of several variables with inequalities as side constraints. *M. Sc. Dissertation. Dept. of Mathematics, Univ. of Chicago*, 1939.
- H. W. Kuhn and A. W. Tucker. Nonlinear programming. In *Traces and emergence of nonlinear programming*, pages 247–258. Springer, 2014.



- A. S. Lewis. Active sets, nonsmoothness, and sensitivity. *SIAM Journal on Optimization*, 13(3):702–725, 2002.
- A. S. Lewis and J. Malick. Alternating projections on manifolds. *Mathematics of Operations Research*, 33(1):216–234, 2008.
- A. S. Lewis, J. Liang, and T. Tian. Partial smoothness and constant rank. *SIAM Journal on Optimization*, 32(1):276–291, 2022.
- Y. Li, Z. Wen, C. Yang, and Y.-x. Yuan. A semismooth Newton method for semidefinite programs and its applications in electronic structure calculations. *SIAM Journal on Scientific Computing*, 40(6):A4131–A4157, 2018.
- J. Liang, J. Fadili, and G. Peyré. Activity identification and local linear convergence of forward–backward-type methods. *SIAM Journal on Optimization*, 27(1):408–437, 2017.
- L. Liang, D. Sun, and K.-C. Toh. A squared smoothing Newton method for semidefinite programming. *arXiv preprint arXiv:2303.05825*, 2023.
- Y. Liu, Z. Wen, and W. Yin. A multiscale semi-smooth Newton method for optimal transport. *Journal of Scientific Computing*, 91(2):39, 2022.
- R. Mifflin. Semismooth and semiconvex functions in constrained optimization. *SIAM Journal on Control and Optimization*, 15(6):959–972, 1977.
- A. Milzarek. *Numerical methods and second order theory for nonsmooth problems*. PhD thesis, Technische Universität München, 2016.
- R. D. Monteiro, C. Ortiz, and B. F. Svaiter. A first-order block-decomposition method for solving two-easy-block structured semidefinite programs. *Mathematical Programming Computation*, 6(2):103–150, 2014.
- B. S. Mordukhovich and N. M. Nam. Geometric approach to convex subdifferential calculus. *Optimization*, 66(6):839–873, 2017.
- Y. Nesterov and A. Nemirovskii. *Interior-point polynomial algorithms in convex programming*. SIAM, 1994.
- J. Nie and L. Wang. Regularization methods for SDP relaxations in large-scale polynomial optimization. *SIAM Journal on Optimization*, 22(2):408–428, 2012.
- J. Nie and L. Wang. Semidefinite relaxations for best rank-1 tensor approximations. *SIAM Journal on Matrix Analysis and Applications*, 35(3):1155–1179, 2014.
- J. Peng and Y. Wei. Approximating k-means-type clustering via semidefinite programming. *SIAM Journal on Optimization*, 18(1):186–205, 2007.
- R. T. Rockafellar and R. J.-B. Wets. *Variational Analysis*, volume 317. Springer Science & Business Media, 2009.

- N. J. A. Sloane. Challenge problems: Independent sets in graphs. <http://www.research.att.com/~njas/doc/graphs.html>, 2005.
- J. F. Sturm. Using SeDuMi 1.02, a MATLAB toolbox for optimization over symmetric cones. *Optimization methods and software*, 11(1-4):625–653, 1999.
- D. Sun, K.-C. Toh, and L. Yang. A convergent 3-block semiproximal alternating direction method of multipliers for conic programming with 4-type constraints. *SIAM Journal on Optimization*, 25(2):882–915, 2015.
- D. Sun, K.-C. Toh, Y. Yuan, and X.-Y. Zhao. SDPNAL+: A matlab software for semidefinite programming with bound constraints (version 1.0). *Optimization Methods and Software*, 35(1):87–115, 2020.
- A. Tavakoli, A. Pozas-Kerstjens, P. Brown, and M. Araújo. Semidefinite programming relaxations for quantum correlations. *Reviews of Modern Physics*, 96(4):045006, 2024.
- K.-C. Toh, M. J. Todd, and R. H. Tütüncü. SDPT3— A MATLAB software package for semidefinite programming, version 1.3. *Optimization methods and software*, 11(1-4):545–581, 1999.
- M. Trick, V. Chvatal, B. Cook, D. Johnson, C. McGeoch, and R. Tarjan. The Second DIMACS Implementation Challenge: NP Hard Problems: Maximum Clique, Graph Coloring, and Satisfiability. *Rutgers University, New Brunswick, NJ*, 1992.
- Y. Wang, K. Deng, H. Liu, and Z. Wen. A decomposition augmented Lagrangian method for low-rank semidefinite programming. *SIAM Journal on Optimization*, 33(3):1361–1390, 2023.
- Z. Wen, D. Goldfarb, and W. Yin. Alternating direction augmented Lagrangian methods for semidefinite programming. *Mathematical Programming Computation*, 2(3):203–230, 2010.
- H. Wolkowicz, R. Saigal, and L. Vandenberghe. *Handbook of semidefinite programming: theory, algorithms, and applications*, volume 27. Springer Science & Business Media, 2012.
- X. Xiao, Y. Li, Z. Wen, and L. Zhang. A regularized semi-smooth Newton method with projection steps for composite convex programs. *Journal of Scientific Computing*, 76(1):364–389, 2018a.
- Y. Xiao, L. Chen, and D. Li. A generalized alternating direction method of multipliers with semi-proximal terms for convex composite conic programming. *Mathematical Programming Computation*, 10(4):533–555, 2018b.
- J. Xu, S. Zhu, Y. C. Soh, and L. Xie. Augmented distributed gradient methods for multi-agent optimization under uncoordinated constant stepsizes. In *54th IEEE Conference on Decision and Control (CDC)*, pages 2055–2060. IEEE, 2015.

- L. Yang, D. Sun, and K.-C. Toh. SDPNAL+: A majorized semismooth Newton-CG augmented Lagrangian method for semidefinite programming with nonnegative constraints. *Mathematical Programming Computation*, 7(3):331–366, 2015.
- M.-C. Yue, Z. Zhou, and A. M.-C. So. A family of inexact SQA methods for non-smooth convex minimization with provable convergence guarantees based on the Luo–Tseng error bound property. *Mathematical Programming*, 174(1-2):327–358, 2019.
- X.-Y. Zhao, D. Sun, and K.-C. Toh. A Newton-CG augmented Lagrangian method for semidefinite programming. *SIAM Journal on Optimization*, 20(4):1737–1765, 2010.